Prediction of soil organic and inorganic carbon concentrations in Tunisian samples by mid-infrared reflectance spectroscopy using a French national library

Cécile Gomez, Tiphaine Chevallier, Patricia Moulin, Imane Bouferra, Kaouther Hmaidi, Dominique D. Arrouays, Claudy C. Jolivet, Bernard Barthès

Prediction of soil organic and inorganic carbon concentrations in Tunisian samples by mid-infrared reflectance spectroscopy using a French national library

Cécile Gomez [1,2], Tiphaine Chevallier [3], Patricia Moulin [4], Imane Bouferra [3], Kaouther Hmaidi [3,5], Dominique Arrouays [6], Claudy Jolivet [6], Bernard G. Barthès [3]

[1] LISAH, University of Montpellier, INRAE, IRD, Montpellier SupAgro, 34060 Montpellier, France. Corresponding author. cecile.gomez@ird.fr

[2] Indo-French Cell for Water Sciences, IRD, Indian Institute of Science, Bangalore 560012, India

[3] Eco&Sols, University of Montpellier, CIRAD, INRAE, IRD, Montpellier SupAgro, 34060 Montpellier, France

[4] US IMAGO, IRD, BP1386, Dakar, Senegal

[5] UR Pédologie, Faculté des Sciences de Tunis, El Manar Tunis, Tunisia

[6] INRAE, US 1106 InfoSol, F45000, Orléans, France

Keywords: Soil Organic and Inorganic Carbon; Mid-Infrared reflectance spectroscopy; natural logarithm transformation; Local and Global calibration; Partial least squares regression (PLSR); National dataset.

Abstract

Mid-infrared reflectance spectroscopy (MIRS, 4000–400 cm^{-1}) is being considered to provide accurate estimations of soil properties, including soil organic carbon (SOC) and soil inorganic carbon (SIC) contents. This approach has mainly been demonstrated by using datasets originating from the same area *A*, with similar geopedological conditions, to build, validate and test prediction models. The objective of this study was to analyse how MIRS performs when applied to predict SOC and SIC contents, from a calibration database collected over a region *A*, to predict over a region *B,* where *A* and *B* have no common area and different soil and climate conditions. This study used a French MIRS soil dataset including 2178 topsoil samples to calibrate SIC and SOC prediction models with partial least squares regression (PLSR), and a Tunisian MIRS topsoil dataset including 96 soil samples to test them. Our results showed that when using the French MIRS soil database, *i)* the SOC and SIC of French validation samples were successfully predicted using global models (R^2_{val} = 0.88 and 0.98, respectively), *ii)* the SIC of Tunisian samples was also predicted successfully both using a global model and using a selection of spectral neighbours from the French calibration database (R^2_{test} of 0.96 for both), *iii)* the SOC of Tunisian samples was predicted moderately by global model (R^2_{test} of 0.64) and a transformation by natural logarithm of the calibration SOC values significantly improved the SOC prediction of Tunisian samples (R^2_{test} of 0.97), and *iv)* a transformation by natural logarithm of SOC values provided more benefit than a selection of spectral neighbours from the French calibration database for predicting Tunisian SOC values. Therefore, in the future, MIRS might replace conventional physico-chemical analysis techniques, or at least be considered as an alternative technique, especially when optimally exhaustive calibration databases will become available.

1. Introduction

Soil is the largest reservoir of continental carbon and participates in the global carbon cycle (Jacobson et al., 2000; Scharlemann et al., 2014). Soil emits carbon dioxide (CO_2) through autotrophic and heterotrophic respiration and acts as a sink of atmospheric CO_2

through photosynthesis; then, organic decomposition products are integrated into the soil as organic matter, which is composed of approximately 50% to 58% of carbon (Gregorich et al., 1994; Pribyl, 2010). Moreover, soil organic carbon (SOC) has a long-acknowledged and key role in soil physical, chemical and biological fertility (Reeves, 1997). Thus, understanding the dynamics of soil carbon is a major issue for soil fertility and for climate change mitigation.

Soil carbon is not only found in organic form. At the global scale, approximately one-third of the total soil carbon is inorganic (soil inorganic carbon, SIC) (Batjes, 1996), and calcareous soils cover more than 30% of the earth's land surface (Chen and Barak, 1982; Romanyà and Rovira, 2011). SIC is mainly in the form of calcium carbonate ($CaCO_3$), and high SIC contents are often localised in dry areas where SOC stocks are low. In these soils, SIC levels can be 2 to 10 times higher than SOC levels (Bernoux and Chevallier, 2014). SIC is made of primary minerals derived from the fragmentation of carbonate bedrock (lithogenic carbonates) or secondary minerals from inorganic carbon precipitation in soil pores or around roots (pedogenic carbonates). Pedogenic carbonates have various forms—nodules, lamellae or crystals—and have varying solubility.

Several analytical methods have been developed to quantify SIC and SOC contents in soils, but they are tedious and/or costly. In particular, SOC determination in carbonated soils often requires hazardous reagents. SIC content has usually been measured by calcimetry (ISO, 1995b) but can also be measured by dry combustion with a CNH elemental analyser equipped with a specific module (CO_3-C module) after phosphoric acid dissolution of the SIC (Mc Crea, 1950; Hannam et al. 2016). Quantifying SOC in calcareous soils has either been carried out directly, by wet oxidation (Walkley and Black, 1934) or dry combustion after removing SIC by acid pretreatment (Harris et al., 2001), or indirectly, by subtracting the SIC, measured by calcimetry, from the total carbon content determined by dry combustion. Due to indirect determination, incomplete oxidation and the use of hazardous reactants with both of these methods, alternative methods based on the thermal lability of SIC and SOC have also been tested (Wang et al., 2012; Apesteguia et al., 2018).

For one to two decades, visible near-infrared (Vis-NIR, 400–2500 nm) and mid-infrared reflectance spectroscopy (MIRS, 4000–400 cm^{-1}), which measures diffuse reflectance, have been proposed as alternative methods to these physico-chemical analytical methods (e.g., Viscarra Rossel et al., 2006; Cécillon et al., 2008; Bellon-Maurel and McBratney, 2011). MIRS is based on the study of absorption bands corresponding to fundamental molecular vibrations, and NIRS is based on the study of absorption bands corresponding to overtones and combinations of fundamental vibrations (Williams and Norris, 1987). Several studies highlighting the potential of Vis-NIR and/or MIRS for predicting various soil attributes, including SIC and SOC, have been listed by Viscarra Rossel et al. (2006) and then by Soriano-Disla et al (2014).

In the MIR range, carbonates may be identified by strong and numerous absorption bands, for instance, bands at approximately 820-750 cm^{-1}, 1800 cm^{-1}, 2520 cm^{-1} and 2900-2990 cm^{-1} (e.g., Tatzber et al., 2007; Du and Zhou, 2009, Comstock et al., 2019). In the NIR range, carbonates may be identified by peaks at 2341 and 2480 nm (Lagacherie et al., 2008; Barthès et al., 2016). In the MIR range, organic carbon may also be identified by numerous absorption peaks, for instance, peaks at approximately 2920 and 1230 cm^{-1} (Grinand et al., 2012). In the NIR range, organic carbon may be identified by absorption peaks at approximately 1910 nm (Viscarra Rossel et al., 2006; Viscarra Rossel and Webster, 2012) and 2050–2150 nm (Workman and Weyer, 2008). Finally, MIRS has generally been reported to provide more accurate performance in terms of SOC and SIC predictions compared to NIRS (e.g., McCarty et al., 2002; Reeves, 2010; Bellon-Maurel & McBratney, 2011; Clairotte et al., 2016). Nevertheless, better NIRS than MIRS predictions of SOC have been reported in tropical and Mediterranean regions due to the overlap of absorption regions related to metal oxides and organic compounds (Rabenarivo et al., 2013; Barthès et al., 2016).

Following the emergence of infrared spectroscopy technologies for soil characterisation, soil spectral libraries covering extensive areas have recently been developed for estimating soil properties, especially SOC; most libraries are in the Vis-NIR range at the national scale (e.g., in Australia, Viscarra Rossel and Webster, 2012; in Denmark, Knadel et al., 2012; in France, Gogé et al., 2014; in China, Shi et al., 2015), continental scale (in Europe, Stevens et al., 2013) and even global scale (Brown et al., 2006; Viscarra Rossel et al., 2016), but libraries also exist in the MIR range (e.g., in France, Grinand et al., 2012, and Clairotte et al., 2016; in the US, Wijewardane et al., 2018, Comstosck et al., 2019 and Dangal et al., 2019). All these libraries use spectra collected using dried and ground samples in laboratory conditions.

Most of the studies dealing with large soil spectral databases (national or continental) have aimed to calibrate prediction models with samples from a region *A* to predict the properties of soil samples from the same region *A*. Therefore, the soil and climate conditions are similar between the calibration and validation databases. McCarty et al. (2002) calibrated SOC and SIC prediction models by using two-thirds of 257 soil samples collected from 14 geographically diverse locations over eight states in the west central US and validated the models by using the remaining one-third of soil samples, obtaining good accuracy and low bias. Stevens et al. (2013) used the LUCAS database, which includes samples from 23 member states of the European Union, to predict SOC. In their study, each calibration dataset and associated validation dataset was composed of samples from a similar soil type (organic or mineral) and land use (cropland, grassland or woodland), and the most spectrally representative samples were selected as calibration samples. Shi et al. (2015) used a Chinese database, which included samples from 20 provinces, to predict SOC. In their study, the calibration dataset was selected to minimise both the spectral distance and geographical distance to each validation sample, which also belonged to the database (region *A*). Clairotte et al. (2016) successfully calibrated prediction models by using subsets of the French national database and then tested these models on a test subset (10% of this French database, either spectrally representative or not; samples were not selected based on their pedo-climatic context).

Some studies have focused on potential and limitation analysis of prediction models calibrated with a large database composed of samples collected over a region *A* to predict properties for soil samples collected from a small region *b* within *A*. McCarty et al. (2002) calibrated SOC and SIC prediction models by using 257 soil samples collected from 14 geographically diverse locations over 8 states in the west central US and obtained biased predictions when their models were applied to 16 independent soil samples collected in another state (Nebraska) that was also in the west central US. Gogé et al. (2014) calibrated local prediction models from the French national database, collected over 550 000 km² (region *A*), to predict soil properties in soil samples collected from a small French area of 24 km² (Occitanie region, south of France; this region *b* was included in *A* but under-represented). Additionally, Comstosck et al. (2019) calibrated prediction models by using a US national database (region *A*) to predict carbonate in soil samples collected from two states (New York and Iowa, regions *b*) that were poorly represented in the US database.

Finally, to the best of our knowledge, few studies have focused on potential and limitation analysis of prediction models calibrated with a large database composed of samples collected over a region *A* to predict properties for soil samples collected over a region *B,* where *A* and *B* have no common area and hence have potential differences in soil and climatic conditions. Only Jauss et al. (2017) and Ahmed et al. (2017) used MIR spectroscopy as a routine method for predicting pyrogenic carbon and for predicting Total

Carbon and SOC, respectively, on United States soils (region *B*), from a soil spectral database of Australia (region *A*).

The objective of this study was to analyse how MIRS may be used to predict SOC and SIC contents when using a national database collected over a region *A* to predict values for soil samples collected over a region *B,* where *A* and *B* have no common area and have different soil and climate conditions. This study used a French MIRS soil dataset (region *A*) including 2178 topsoil samples collected from an area of 550 000 km² (French metropolitan territory, composed of temperate and Mediterranean soils) to calibrate SIC and SOC prediction models. These models were tested on a Tunisian MIRS soil dataset (region *B*), including 96 soil samples collected from an area of approximately 80 000 km² (northern half of Tunisia, mainly Mediterranean and arid soils).

2. Materials and methods

2.1. Soil datasets

2.1.1. The French national soil collection

The national soil collection provided by the French national soil quality monitoring network (RMQS; Arrouays et al., 2002) and called *DB_RMQS* was used in this study to calibrate the SIC and SOC models. This RMQS collection is composed of 2178 soil samples representing all main soil types encountered over the sampled 552 000 km² of the French metropolitan territory (Corsica included): Cambisols, Calcosols, Luvisols, Leptosols, Andosols, Albeluvisols, Podzosols, *etc.* (IUSS Working Group WRB, 2014). The latitude of sample sites ranges from 41 to 51°N, and their longitude ranges from 5.0°W to 9.5°E. The sampling design was based on a square grid with 16-km spacing. At the centre of each square, 25 individual core samples were taken from 0 to 30 cm depth using an unaligned sampling design within a 20 × 20 m area. Core samples were bulked to obtain a composite sample for each site (Arrouays et al., 2002).

2.1.2. The Tunisian soil samples

Ninety-six soil samples were used as the test set, called *DB_Tunisia*. These samples were collected from 45 localities, covering approximately 80 000 km² (from 35 to 37°N and 08 to 11°E), with the aim of representing the main soil types and land uses of the northern half of Tunisia. This was done based on previous studies carried out at the Tunis El Manar University, without particular design. Field samples within the same locality were kilometres apart and under different land uses. Soil samples were collected at 0-10 cm using a spade, and the sampling campaign was carried out within a few months in late 2010. This Tunisian set was previously studied in Barthès et al. (2016).

2.2. Laboratory Analysis

2.2.1. Physico-chemical analyses

The 2178 RMQS samples were air dried, 2-mm sieved and then finely ground (< 0.25 mm) using mortar and pestle. The SIC content of the RMQS samples was calculated as 0.12 times the soil calcium carbonate content, which was determined using these finely ground (< 0.25 mm) air-dried samples using a Bernard calcimeter according to the standard procedure ISO 10693 (ISO, 1995a). The carbonate content was calculated after calibration with a pure calcium carbonate standard and was expressed as the equivalent calcium carbonate content. The SIC content of the RMQS samples (*DB_RMQS_SIC*) ranged from 0 to 103.9 g kg^{-1}, averaged 6.4 g kg^{-1}, and had a median of 0 g kg^{-1} and a skewness value close to 3.1 (Table 1).

Then, the SOC content of the RMQS samples was calculated as the difference between the total carbon (TC) and inorganic carbon contents. The TC content was determined by dry combustion with an elemental analyser (Thermo Fisher Scientific CHN NA2000, Waltham, MA, US) using approximately 25–30-mg aliquots of finely ground (< 0.25 mm) air-dried soil samples that were sealed into tin capsules, according to the standard procedure ISO 10694 (ISO, 1995b). The SOC content of the RMQS samples (*DB_RMQS_SOC*) ranged from 0.6 to 411.3 g kg^{-1}, averaged 25.8 g kg^{-1}, and had a median of 19.6 g kg^{-1} and a skewness value close to 4.9 (Table 1).

[Table 1]

The 96 Tunisian soil samples were also air-dried, sieved to 2 mm and then finely ground (< 0.2 mm) using mortar and pestle. The SOC content of the Tunisian samples was analysed by dry combustion after decarbonisation using chlorhydric acid, following the standard procedure ISO 10694 (1995b), with the same elemental analyser as that used for RMQS samples but using silver capsules. Soils were decarbonated prior to SOC determination: 10 mL of water were added to 1 g of soil and 0.5 M HCl solution was then dripped onto the sample until there was no more effervescence; then the samples were washed in water until pH reached 7. The SOC concentration was then determined on finely ground 25–30 mg aliquots by dry combustion using an elemental analyser (Thermo Fisher Scientific CHN NA2000, Waltham, MA, USA). The SOC content of the Tunisian samples (*DB_Tunisia_SOC*) ranged from 2.0 to 121.0 g kg^{-1}, averaged 20.1 g kg^{-1}, and had a median of 14.6 g kg^{-1} and a skewness value close to 3 (Table 1).

The soil inorganic carbon content of the Tunisian samples was calculated as the difference between the TC (determined by dry combustion using the same CHN analyser as that used for the RMQS samples) and SOC contents. The SIC content of the Tunisian samples (*DB_Tunisia_SIC*) ranged from 0.0 to 92.9 g kg^{-1}, averaged 43.3 g kg^{-1}, and had a skewness value close to -0.2 (Table 1).

As the SIC contents of the RMQS and Tunisian samples were analysed by two different methods, 29 test samples from the Tunisian set (i.e., 30% of the set) were re-analysed following the same method as that used for the RMQS samples (i.e., directly, by calcimetry; ISO, 1995a). The Pearson correlation coefficient (R), root mean square error (RMSE) and bias between the SIC values determined by both approaches (calcimetry vs. difference between TC and SOC) were 0.997, 2.4 g kg^{-1} and 1.1 g kg^{-1}, respectively (Figure 1). The values of SIC calculated by both approaches could thus be considered equivalent.

[Figure 1]

2.2.2. Mid-infrared spectroscopy

Mid-infrared spectroscopic analysis was performed following the same procedure for both spectral libraries. First, air-dried, 2-mm sieved, and 0.2-mm ground samples were oven-dried at 40°C for twelve hours. Reflectance spectra were acquired using a Fourier transform Nicolet 6700 spectrophotometer (Thermo Fischer Scientific, Madison, WI, US) in the MIR region. Reflectance was acquired at 934 wavenumbers between 4000 and 400 cm^{-1} with a 3.86 cm^{-1} spectral resolution. This spectrophotometer is equipped with a silicon carbide source, a Michelson interferometer as a dispersive element, and a deuterated triglycine sulfate detector. Soil samples were placed in a 17-well plate. The soil surface was flattened with the flat section of a glass cylinder, and samples were then scanned using an auto-sampler (soil surface area scanned: ca. 10 mm^2). Each spectrum resulted from 32 co-added scans, and the body of the plate (next to the wells) was used as a reference standard and scanned once per plate (i.e., every 17 samples). Twenty wavenumbers were removed due to frequent noise in the spectrum, so MIR spectra in the range from 4000 to 478 cm^{-1}, with 914 wavenumbers, were used.

2.3 PLSR model calibration

All procedures were performed using R software (R Core Team, 2012), and both the ade4 (Dray and Dufour, 2007) and pls packages (Mevik and Wehrens, 2007) were used.

2.3.1. Dataset preparation

Both *DB_RMQS_SIC* and *DB_RMQS_SOC* were divided into a calibration set (3/4 of the dataset) and a validation set (1/4 of the dataset). The samples of each dataset were ranked according to ascending reference value (observed SIC or SOC). The sample with the lowest reference value was put in the calibration set, the next sample was put in the validation set, and then the next three samples were put in the calibration set. The procedure was continued by alternately placing the next sample in the validation set and the following three samples in the calibration set. Following this process, the distributions of the *DB_Calib_RMQS_SOC* calibration and *DB_Valid_RMQS_SOC* validation datasets were similar. As well, the distributions of the *DB_Calib_RMQS_SIC* calibration and *DB_Valid_RMQS_SIC* validation datasets were similar.

As the SOC values of the RMQS dataset followed a non-normal distribution (Table 1), the SOC values of the *DB_Calib_RMQS_SOC* calibration dataset were transformed with natural logarithm (ln(SOC)) to reach a normal distribution, giving rise to new dataset for calibration *DB_Calib_RMQS_lnSOC*. The SIC distribution in the French dataset was also non normal, but due to the very large number of null values, ln-transformation was hardly possible (Bellon-Maurel et al., 2010; Terra et al., 2015).

The reflectance was converted into "absorbance" ($\log_{10}$ [1/reflectance]), and a standard normal variate correction was applied to remove additive and multiplicative effects (Barnes et al., 1989). Spectral outliers, which are defined as samples spectrally different than the rest of the samples (e.g., Pearson, 2002), were removed from the calibration datasets. The spectral outliers were identified by applying the Mahalanobis distance (Mark and Tunnell, 1985) to data condensed by principal component analysis (PCA). In the present study, a Mahalanobis distance of 3.5 was selected as the threshold for the identification of spectral outliers.

2.3.2. Partial least squares regression

Partial least squares regression (PLSR) is a multivariate approach that specifies a linear relationship between a dependent (response) variable (Y-variable, i.e., SIC or SOC content in the present case), and a set of predictor variables (X-variables, i.e., MIR spectra in the present case; Tenenhaus, 1998). The general concept of PLSR is to extract a small number of orthogonal variables (called the latent variables) that account for the maximum variation in the X-variables. A detailed description of the PLSR procedure can be found in Wold et al. (2001). This method is commonly used for NIRS or MIRS prediction of soil properties (e.g., Viscarra-Rossel et al., 2006; Bellon-Maurel et al, 2010).

The maximum number of latent variables of PLSR was defined as 30. A leave-one-out cross-validation (LOOCV) procedure was adopted to verify the prediction capability of the PLSR model for the calibration set. Each time, $n - 1$ samples were used to build a regression model, which was applied to the sample not used in developing the model. This procedure was repeated for all n samples, resulting in predictions for all n samples.

2.3.3. Global models

Global calibration is a common calibration procedure where all calibration samples are used to build a unique prediction model that is applied identically to all validation or test samples. One global prediction model (denoted GM_{SIC}) was built for SIC prediction based on *DB_Calib_RMQS_SIC,* validated on *DB_Valid_RMQS_SIC* and tested on *DB_Tunisia_SIC.* As well, a global prediction model (denoted GM_{SOC}) was built for SOC prediction based on *DB_Calib_RMQS_SOC*, validated on *DB_Valid_RMQS_SOC* and tested on *DB_Tunisia_SOC*. Finally, a global prediction model (denoted GM_{lnSOC}) was built for SOC prediction based on *DB_Calib_RMQS_lnSOC,* applied to spectra of *DB_Valid_RMQS_SOC* and *DB_Tunisia_SOC*, and the output predictions ln(SOC) were back-transformed into SOC values using exp(ln(SOC)).

The optimal number of latent variables of GM_{SIC}, GM_{SOC} and GM_{lnSOC} was determined using prediction residual error sum of squares (PRESS) analysis of LOOCV results to avoid under- and over-fitting. Then, all calibration samples were used to build the prediction model with the appropriate number of latent variables, and this model was applied to validation and test sets.

2.3.4. Local models

A local regression approach was implemented based on PLSR to predict the SOC and SIC content of Tunisian samples. Given a sample p_i from *DB_Tunisia* to predict:

1- The Pearson coefficient of correlation between the spectrum of the Tunisian sample p_i and each RMQS calibration spectrum (from *DB_Calib_RMQS)* was calculated;

2- The *N* samples from *DB_Calib_RMQS* with spectra that correlated to the spectrum of p_i beyond a cut-off value of 0.95 were considered spectral neighbours of the Tunisian sample p_i, without maximum limit for *N*.

3- A PLSR model was built using the *N* spectral neighbours of the Tunisian sample p_i.

If a Tunisian soil sample had less than 30 spectral neighbours among the *DB_Calib_RMQS* set, this soil sample was not predicted.

One local prediction model (denoted LM_{SIC}) was built for SIC prediction based on *DB_Calib_RMQS_SIC,* validated on *DB_Valid_RMQS_SIC* and tested on *DB_Tunisia_SIC.* One local prediction model (denoted LM_{SOC}) was built for SOC prediction based on *DB_Calib_RMQS_SOC,* validated on *DB_Valid_RMQS_SOC* and tested on *DB_Tunisia_SOC*. Finally, one local prediction model (denoted LM_{lnSOC}) was built for SOC prediction based on *DB_Calib_RMQS_lnSOC,* applied to spectra of *DB_Valid_RMQS_SOC* and *DB_Tunisia_SOC*, and the output predictions ln(SOC) were back-transformed into SOC values using exp(ln(SOC)).

As the calibration sets for SOC and SIC predictions did not include the same samples (*DB_Calib_RMQS_SOC* and *DB_Calib_RMQS_SIC*, respectively), the nearest calibration neighbours of a given French validation and Tunisian sample were not the same for SOC and SIC predictions. The optimal number of latent variables was finally determined using PRESS analysis of LOOCV on the selected spectral neighbours to avoid under- and over-fitting. Regardless of the type of local model, the spectral outliers were not investigated because the selection of nearest neighbours was considered an implicit rejection of outliers.

2.4 PLSR model evaluation

The performance of global models was evaluated according to figures of merit described in Bellon Maurel et al. (2010), from cross-validation, validation and test databases.

The coefficient of determination of cross-validation (R^2_{cv}) and root mean square error of cross-validation (*RMSECV*) for *DB_Calib_RMQS* were used. R^2_{cv} was computed as 1-ESS/TSS, where ESS is the error sum of squares and TSS the total sum of squares.

The coefficient of determination and root mean square error of prediction for *DB_Valid_RMQS*, R^2_{val} and $RMSE_{val}$ respectively, were used. R^2_{val} was also computed as 1-ESS/TSS. The ratio of performance to deviation in *DB_Valid_RMQS* (RPD_{val}), which is the ratio between the standard deviation in *DB_Valid_RMQS* and $RMSE_{val}$, was calculated. The ratio of performance to interquartile range of *DB_Valid_RMQS* ($RPIQ_{val}$), which is the ratio between interquartile range (difference between the third and first quartiles) of *DB_Valid_RMQS* and $RMSE_{val}$, was also calculated. This parameter has been proposed for variables with non-normal distributions (Bellon-Maurel et al., 2010). And the bias, which is the mean difference between observations and predictions, was calculated for *DB_Valid_RMQS* ($bias_{val}$).

The coefficient of determination and root mean square error of prediction for *DB_Tunisia*, R^2_{test} and $RMSE_{test}$ respectively, were used. R^2_{test} was computed as 1-ESS/TSS. The ratio of performance to deviation in *DB_Tunisia* (RPD_{test}), which is the ratio between the standard deviation in *DB_Tunisia* and $RMSE_{test}$, was calculated. The ratio of performance to interquartile range of *DB_Tunisia* ($RPIQ_{test}$), which is the ratio between the interquartile range of *DB_Tunisia* and $RMSE_{test}$, was also calculated. And the bias, which is the mean difference between observations and predictions, was calculated for *DB_Tunisia* ($bias_{test}$).

Finally, a wavelength was considered a significant contributor in a global model when the values of both the regression coefficient and variable importance in the projection (VIP) were sufficiently large: the threshold for the VIP was set to 1 (Chong and Jun, 2005; Wold et al., 1993, 2001), and the thresholds for the regression coefficients were their standard deviations (Viscarra-Rossel et al., 2008).

The performances of local models were based on the same figures of merit as those used in global calibration, calculated on *DB_Valid_RMQS and DB_Tunisia.*

Concerning the models built from the *DB_Calib_RMQS_lnSOC,* independent validation and test statistics were calculated from back-transformed data.

4. Results

4.1. Preliminary analysis of soil properties and spectra

The RMQS soil sampling covered the French territory, and ranges of SOC and SIC contents in the *DB_RMQS_SOC* and *DB_RMQS_SIC*, respectively, are large (Table 1). According to the French soil classification, 33 soil reference groups were sampled, with a dominance of Cambisols (IUSS Working Group WRB, 2014; 27% of the sample set), calcareous soils (Calcosols, 22%) and Luvisols (16%). High SIC values are mainly located in three French areas: 1) the southeast (Prealps), mainly with Leptosols and Calcosols, 2) the northeast (chalk Champagne) also mainly with Leptosols, and 3) a transect from west (the Aquitanian Basin) to south (Mediterranean Sea), mainly with Calcosols (Figure 2A1). High SOC values are mainly located in 1) mountain areas (Alps in the southeast, Pyrenees in the extreme southwest, Massif Central in the south-centre, Jura in the centre-east), 2) cool regions covered by forests and pastures (centre-east), and 3) intensive livestock production areas (northwest; Figure 2B1).

The Tunisian soil samples covered the northern half of Tunisian territory, and the SIC contents range in the *DB_Tunisia_SIC* is as large as the one in the *DB_RMQS_SIC*, whereas the SOC contents range in the *DB_Tunisia_SOC* is lower than the one of the *DB_RMQS_SOC* (Table 1). The sampled Tunisian soils were mainly Calcaric Cambisols and Regosols, Kastanozems, and Chromic and Vertic Cambisols.

[Figure 2]

Principal component analyses were performed on pre-treated spectra of *DB_Calib_RMQS_SIC* and *DB_Calib_RMQS_SOC*, respectively, and pre-treated Tunisian spectra were projected onto the plans made by the first and second components. Most Tunisian spectra overlapped a subset of RMQS spectra for SIC (Figure 3a) and for SOC (Figure 3b). So most Tunisian soil samples had similar spectral signatures than a subset of RMQS spectra used for calibrating prediction models.

[Figure 3]

4.2. Global models

a. Soil inorganic carbon content

For SIC prediction, 52 spectral outliers were identified within the initial calibration dataset, so 1582 RMQS samples were ultimately kept and constituted the *DB_Calib_RMQS_SIC* dataset. The SIC content of these 1582 RMQS samples contained in *DB_Calib_RMQS_SIC* ranged from 0.0 to 103.9 g kg^{-1}, averaged 6.4 g kg^{-1}, and had a skewness value close to 3.1 (Table 1). The SIC content of the 544 RMQS samples contained in *DB_Valid_RMQS_SIC* ranged from 0.0 to 95.2 g kg^{-1}, averaged 6.3 g kg^{-1}, and also had a skewness value close to 3.1 (Table 1).

The GM_{SIC} was built from the *DB_Calib_RMQS_SIC* dataset using an optimal number of 15 latent variables, validated on the *DB_Valid_RMQS_SIC* dataset and then tested on the *DB_Tunisia_SIC* dataset. The performance of the GM_{SIC} prediction model was accurate, with an R^2_{cv} of 0.97 and $RMSECV$ of 2.8 g kg^{-1} in the calibration step (Table 2) and an R^2_{val} of 0.98 and $RMSE_{val}$ of 2.1 g kg^{-1} in the validation step (Table 2, Figure 4b). When applied to the *DB_Tunisia_SIC* dataset, this GM_{SIC} prediction model provided accurate and unbiased predictions (R^2_{test} = 0.96, $RMSE_{test}$ = 5.2 g kg^{-1} and $bias_{test}$ = 0.2 g kg^{-1}; Table 3, Figure 4c).

A total of 96 spectral bands might be considered significant based on the analysis of the VIP and regression coefficients of GM_{SIC} (Figure 4d). Among the 96 significant spectral bands, those at approximately 2500, 1800 and 860 cm^{-1} had regression coefficients higher than 3 times the standard deviation and therefore might be considered the most significant ones.

[Figure 4]

[Table 2]

[Table 3]

b. Soil organic carbon content

For SOC prediction, 48 spectral outliers were identified within the initial calibration dataset, so 1586 RMQS samples were ultimately kept and constituted the *DB_Calib_RMQS_SOC* and *DB_Calib_RMQS_lnSOC* datasets. The SOC contents of the 1586 RMQS samples of *DB_Calib_RMQS_SOC* ranged from 0.6 to 411.3 g kg^{-1}, averaged 25.6 g kg^{-1}, and had a skewness value close to 5.5 (Table 1). The ln(SOC) values of the 1586 RMQS samples of *DB_Calib_RMQS_lnSOC* ranged from -0.5 to 6 ln(g kg^{-1}), averaged 3 ln(g kg^{-1}), had a median of 3 ln(g kg^{-1}) and a skewness value close to 0.3. The SOC content of the 544 RMQS samples contained in *DB_Valid_RMQS_SOC* ranged from 1.5 to 159 g kg^{-1}, averaged 25.5 g kg^{-1}, and had a skewness value close to 2.5 (Table 1).

The GM_{SOC} was built from the *DB_Calib_RMQS_SOC* dataset using 23 latent variables, validated on the *DB_Valid_RMQS_SOC* dataset and then tested on the *DB_Tunisia_SOC* dataset. The performance of the GM_{SOC} prediction model was modest, with an R^2_{cv} of 0.80 and *RMSECV* of 9.9 g kg^{-1} in the calibration step (Table 2) and an R^2_{val}

of 0.88 and $RMSE_{val}$ of 7.2 g kg^{-1} in the validation step (Table 2, Figure 5b). When applied to the Tunisian test set, this GM_{SOC} prediction model provided low accuracy (R^2_{test} = 0.64, $RMSE_{test}$ = 16.0 g kg^{-1}) and biased predictions ($bias_{test}$ = -5.2 g kg^{-1}) (Table 3, Figure 5c).

A total of 92 spectral bands might be considered significant based on the analysis of the VIP and regression coefficients of GM_{SOC} (Figure 5d). Nevertheless, among these 92 spectral bands, none was associated to very high regression coefficients.

[Figure 5]

A GM_{lnSOC} prediction model was built from the *DB_Calib_RMQS_lnSOC* dataset using 10 latent variables and this model was applied to spectra of both *DB_Valid_RMQS_SOC* and *DB_Tunisia_SOC* datasets. Finally, the ln(SOC) predictions were back-transformed into SOC values for calculating the figures of merit. The performance of the GM_{lnSOC} prediction model was accurate, with an R^2_{cv} of 0.89 and *RMSECV* of 0.2 g kg^{-1} in the calibration step (Table 2) and an R^2_{val} of 0.90 and $RMSE_{val}$ of 6.6 g kg^{-1} in the validation step (Table 2, Figure 6b). When applied to the Tunisian test set, the GM_{lnSOC} prediction model provided high accuracy (R^2_{test} = 0.97, $RMSE_{test}$ = 4.2 g kg^{-1}) and very slightly biased predictions ($bias_{test}$ = 0.7 g kg^{-1}) (Table 3, Figure 6c).

A total of 95 spectral bands might be considered significant based on the analysis of the VIP and regression coefficients in the GM_{lnSOC} (Figure 6d). Among these 95 significant spectral bands, those at approximately 2915, and 1800 cm^{-1} had regression coefficients higher than 3 times the standard deviation and therefore might be considered the most significant ones.

[New Figure 6]

4.3. Local models

a. Soil inorganic carbon content

All validation soil samples had more than 30 spectral neighbours within the *DB_Calib_RMQS_SIC* dataset, so SIC could be predicted from LM_{SIC} for all samples of *DB_Valid_RMQS_SIC.* The LM_{SIC} provided very accurate and unbiased SIC predictions in validation (R^2_{val} = 0.99 and $RMSE_{val}$ = 1.8 g kg^{-1}; Table 2). Therefore, this LM_{SIC} provided validation performance slightly better than that of GM_{SIC} (Table 2).

All Tunisian soil samples had more than 30 spectral neighbours within the *DB_Calib_RMQS_SIC* dataset, so SIC could be predicted from LM_{SIC} for all Tunisian samples. The LM_{SIC} provided accurate and slightly biased SIC predictions on Tunisian samples (R^2_{test} = 0.96, $RMSE_{test}$ = 5.6 g kg^{-1} and $bias_{test}$ = 1.7 g kg^{-1}; Table 3, Figure 7a). Therefore, LM_{SIC} provided test performance slightly lower than that of GM_{SIC}, mainly due to bias (Table 3). The number of latent variables selected for LM_{SIC} on Tunisian samples varied depending on the sample predicted and followed a relatively normal distribution centred at approximately 13, which was close to the optimal number of latent variables selected by the GM_{SIC} (Figure 7c).

The number of spectral neighbours of Tunisian samples varied from 65 to 1293 (Figure 7b). Only a slight trend was observed between the number of neighbours and the prediction error, with a lower error when the number of neighbours increased (Figure 7b). This trend could be expected, as the use of a higher number of neighbour samples for calibration should result in more accurate predictions. The spectra from *DB_Calib_RMQS_SIC* used for building the 96 local individual Tunisian models LM_{SIC} were selected from 0 to 87 times. So no spectrum from *DB_Calib_RMQS_SIC* was systematically selected, whereas only 1.6% of spectra from *DB_Calib_RMQS_SIC* were never selected. The frequently selected samples were mainly located in SIC-richest areas (Calcosols and Leptosols) such as the southeast (Prealps), the northeast (chalk

Champagne) and the transect from west (the Aquitanian Basin) to south (Mediterranean Sea) (Figure 2A1 and 2A2).

[Figure 7]

b. Soil organic carbon content

As *DB_Calib_RMQS_SOC* and *DB_Calib_RMQS_lnSOC* datasets contained same predictors X-variables (MIR spectra), spectral neighbours of validation samples were the same for LM_{SOC} and LM_{lnSOC} models. All validation soil samples had more than 30 spectral neighbours within the *DB_Calib_RMQS_SOC* dataset and *DB_Calib_RMQS_lnSOC* datasets, so SOC and ln(SOC) could be predicted from LM_{SOC} and LM_{lnSOC}, respectively, for all samples of *DB_Valid_RMQS_SOC.* The LM_{SOC} provided accurate and very slightly biased SOC predictions in validation (R^2_{val} = 0.93, $RMSE_{val}$ = 5.4 g kg^{-1} and $bias_{val}$ = -0.7 g kg^{-1}; Table 2). Therefore, LM_{SOC} provided validation performance higher than that of GM_{SOC} (Table 2). The LM_{lnSOC} provided accurate and unbiased SOC predictions in validation (R^2_{val} = 0.92, $RMSE_{val}$ = 5.7 g kg^{-1} and $bias_{val}$ = -0.1 g kg^{-1}; Table 2). Therefore, LM_{lnSOC} provided validation performance higher than that of GM_{SOC} and almost similar to that of LM_{SOC} (Table 2).

All Tunisian soil samples also had more than 30 spectral neighbours within the *DB_Calib_RMQS_SOC* and *DB_Calib_RMQS_lnSOC* datasets, so SOC and ln(SOC) could be predicted from LM_{SOC} and LM_{lnSOC}, respectively, for all Tunisian samples. The LM_{SOC} provided accurate and very slightly biased SOC predictions on Tunisian samples (R^2_{test} = 0.89, $RMSE_{test}$ = 6.9 g kg^{-1} and $bias_{test}$ = 0.5 g kg^{-1}; Table 3, Figure 8a). Therefore, this LM_{SOC} provided test performance markedly higher than that of GM_{SOC} (Table 3). The number of latent variables selected by this LM_{SOC} depending on the sample followed a bimodal distribution centred at approximately 16 and 22 (Figure 8c). The second peak of number of latent variables, approximately 22, was close to the number of latent variables selected by the *GM_{SOC}* (Figure 8c).

The *LM_{lnSOC}* model provided accurate and very slightly biased SOC predictions on Tunisian samples (R^2_{test} = 0.93, $RMSE_{test}$ = 5.8 g kg^{-1} and $bias_{test}$ = -0.6 g kg^{-1}; Table 3, Figure 9a). The *LM_{lnSOC}* provided test performance markedly higher than that of *GM_{SOC}* but lower than that of *GM_{lnSOC}* (Table 3). The number of latent variables selected by this *LM_{lnSOC}* depending on the sample followed a relatively normal distribution centred at approximately 11 (Figure 9c), which was close to the optimal number of latent variables selected by the *GM_{lnSOC}*.

As *DB_Calib_RMQS_SOC* and *DB_Calib_RMQS_lnSOC* datasets contained same predictors X-variables (MIR spectra), spectral neighbours of Tunisian samples were the same for *LM_{SOC}* and *LM_{lnSOC}* models. The number of spectral neighbours of Tunisian samples varied from 65 to 1292 (Figure 8b and 9b), and no clear trend was observed between the number of neighbours and the prediction error obtained by *LM_{SOC}* and *LM_{lnSOC}* models (Figure 8b and 9b, respectively). As for SIC prediction with *LM_{SIC}*, the spectra from *DB_Calib_RMQS_SOC* and *DB_Calib_RMQS_lnSOC* datasets used for building the 96 individual local Tunisian models were selected from 0 to 87 times. So no spectrum from *DB_Calib_RMQS_SOC* and *DB_Calib_RMQS_lnSOC* datasets was systematically selected, whereas 1.7% of spectra from *DB_Calib_RMQS_SOC* and *DB_Calib_RMQS_lnSOC* datasets were never selected. The frequently selected samples were mainly located in SOC-poor areas (Calcosols and Leptosols) in the northeast (chalk Champagne) and on the transect from west (Aquitanian Basin) to south (Mediterranean Sea) and in soils richer in SOC in the southeast (Prealps) (Figure 2B1 and 2B2).

[Figure 8]

[New Figure 9]

5. Discussion

5.1. Global models built on region A for application to region A.

Before being applied to the Tunisian database, the global models were calibrated with an RMQS subset (*DB_Calib_RMQS_SIC, DB_Calib_RMQS_SOC* and *DB_Calib_RMQS_lnSOC*) and validated on an RMQS subset (*DB_Valid_RMQS_SIC* and *DB_Valid_RMQS_SOC*), which means that the global models were calibrated using soil samples collected over a region *A* to predict values for soil samples collected over this same region *A*.

The validation performance of GM_{SIC} was in accordance with results reported in the literature. Grinand et al. (2012) obtained similar performances using the same RMQS MIRS database, with R^2_{val} and RPD_{val} values of 0.97 and 7.6, respectively, when 3/4 of the set, selected at random, was used for calibration and 1/4 was used for validation. Barthès et al. (2016) obtained similar performances for SIC using the Tunisian MIRS database for both calibration and prediction, with R^2_{cv} and RPD_{cv} values of 0.98 and 7.8, respectively. Mc Carty et al. (2002) obtained similar performances using another MIRS database collected in the US, with R^2_{val} = 0.98 (RPD_{val} was not mentioned and could not be calculated). The most significant spectral bands for GM_{SIC}, located at 2500, 1800 and 860 cm^{-1} (Figure 4d), might be attributed to stretching or bending vibrations in carbonate molecules, as suggested by Du and Zhou (2009) and then by Grinand et al. (2012).

The validation performance of the GM_{SOC} was also in accordance with some literature results. Clairotte et al. (2016) obtained very similar performances using the full RMQS MIRS database (including two depth layers, 0-30 and 30-50 cm, instead of one in the present study), with R^2_{val} and RPD_{val} values of 0.88 and 2.7, respectively. Barthès et al.

(2016) obtained better performances using the Tunisian MIRS database with cross-validation, with R^2_{cv} and RPD_{cv} values of 0.95 and 4.3, respectively. Moreover, Mc Carty et al. (2002) obtained slightly higher performances using a MIRS database collected in the US for both SOC calibration and validation, with R^2_{val} = 0.94 (RPD_{val} was not mentioned and could not be calculated).

Following previous researches dealing with non-normal distribution of soil properties (e.g., Waruru et al., 2014; Dangal et al., 2019), natural logarithm transformation was applied to the highly skewed SOC values of the RMQS database to reach a normal distribution in the calibration dataset (*DB_Calib_RMQS_lnSOC)*. Thanks to this normal distribution, the performance of the GM_{lnSOC} on *DB_Valid_RMQS_SOC* was slightly better than the one of the GM_{SOC}.

Finally, validation performance was higher for SIC with GM_{SIC} (R^2_{val} and RPD_{val} values of 0.98 and 7.6, respectively; Table 2) than for SOC prediction with GM_{SOC} (R^2_{val} and RPD_{val} values of 0.88 and 2.7, respectively; Table 2) and GM_{lnSOC} (R^2_{val} and RPD_{val} values of 0.90 and 2.9, respectively; Table 2), confirming that MIRS allows markedly more accurate predictions of SIC than SOC as also shown by McCarty et al. (2002), Grinand et al. (2012) and Barthès et al. (2016).

5.2. Models built on region A for application to region B.

The models were calibrated by using a RMQS subset (*DB_Calib_RMQS_SIC, DB_Calib_RMQS_SOC* and *DB_Calib_RMQS_lnSOC*) and tested on the Tunisian dataset, which means that the models were calibrated by using soil samples collected over a region *A* to predict values for soil samples collected over a region *B*, where *A* and *B* had no common area, so the soil and climate conditions were different between the calibration and test datasets. Our results showed that GM_{SIC} provided accurate test performance (R^2_{test} and RPD_{test} values of 0.96 and 4.9, respectively; Table 3), which was however lower when applied to region *B* than to region *A* (Figure 4c, Tables 2 and 3). The GM_{SOC} also provided markedly lower performance (R^2_{test} and RPD_{test} values of 0.64 and 1.3, respectively; Table 3) when applied to our region *B* than to our region *A* (Figures 5c, Table 2 and 3).

The RMQS spectra used for SIC and SOC predictions by local models were selected using a similarity measure (Pearson's coefficients of correlation), following the same approach than Shenk et al. (1997) and Nocita et al. (2014). So the driver of neighbours selection was the spectral similarity between Tunisian and French spectra. The LM_{SIC} did not improve the SIC prediction accuracy compared to the GM_{SIC} (Table 3). Therefore, GM_{SIC} seemed robust and did not need to be adjusted to spectral particularities of region *B*. So rather than spectral similarity between French and Tunisian samples, the main reason for accurate SIC predictions in region *B* seemed to be the strong spectral features of SIC in the MIR region, as suggested by Gogé et al. (2014). The LM_{SOC} improved SOC prediction accuracy compared to the GM_{SOC} (Table 3). Therefore, GM_{SOC} seemed poorly robust and the calibration over region *A* needed to be adjusted to spectral particularities of region *B* using spectral neighbours (e.g., Shenk et al., 1997; Nocita et al., 2014). The increase in the performance of MIRS-based SOC prediction when shifting from global to local PLSR is in accordance with literature (e.g. Ramirez-Lopez et al., 2013; Shi et al., 2015; Clairotte et al., 2016 and Dangal et al., 2019). Finally, the frequently selected spectral neighbours of Tunisian samples by the LM_{SOC} were mainly located in SOC-poor areas in the northeast (chalk Champagne) and on the transect from west (Aquitanian Basin) to south (Mediterranean Sea) and in soils richer in SOC in the southeast (Prealps) (Figure 2B1 and 2B2). So these frequently selected spectral neighbours of Tunisian samples by SOC local model were not located only over the more similar climatic and pedological contexts such as the Mediterranean context (southeast of France).

5.3. Impact of the SOC ln-transformation on models built on region A for application to region B.

The global model calibrated on region *A* with log-transformed SOC values (GM_{lnSOC}) provided accurate performance on region *B* (R^2_{test} and $RMSE_{test}$ values of 0.97 and 4.9 g kg^{-1}, respectively; Figure 6c, Table 3). The local model provided better performance when calibrated on region *A* with log-transformed SOC values (LM_{lnSOC}) than with SOC values (LM_{SOC}), but less accurate than GM_{lnSOC} on region *B* (R^2_{test} and $RMSE_{test}$ values of 0.93 and 3.6 g kg^{-1}, respectively; Figure 9c, Table 3). So whatever the model using log-transformed SOC data in calibration database (GM_{lnSOC} or LM_{lnSOC}), the SOC predictions on region *B* were improved compared to models using highly skewed SOC values in calibration database (GM_{SOC} or LM_{SOC}; Table 3), as showed by Jaconi et al. (2019).

Finally, and unexpectedly, GM_{lnSOC} provided better performance than LM_{SOC} when applied on Tunisian samples. So a transformation of calibration SOC values improved SOC model performance more clearly than spectral selection of calibration samples (neighbours). Therefore SOC model performance was more sensitive to the distribution of the explained variable of the calibration samples than to spectral similarity between calibration and test spectra.

5.4. Perspectives

This study, which used MIRS to predict SOC and SIC contents by using a database collected over a region *A* to predict values over a region *B*, where *A* and *B* have no common area, could be continued with a study to develop predictions based on selected spectral bands. Indeed, spectral band selection remains to be explored, as several studies testing such an approach have obtained different results. Viscarra Rossel and Lark (2009) successfully used wavelets and a variable selection technique to improve SOC calibration using Vis–NIR and MIRS data. Additionally, Volhand et al. (2016) outperformed SOC predictions based on Vis–NIR spectra by using band selection. However, Stevens et al. (2013) tested recursive feature elimination based on the random forest approach and obtained no overall increase in the accuracy of soil property prediction using the LUCAS (European) Vis-NIR soil database compared to models using all spectral bands. In addition, Yang et al. (2019) tested a generic algorithm for spectral band selection but obtained no overall increase in SOC prediction accuracy. As previously tested by, e.g., Guerrero et al. (2014) and Guy et al. (2016), spiking could be another useful approach to improve prediction accuracy when applying large-scale calibrations to small regions. Spiking consists of adding a small subset of samples from region *B* (spiking subset) to the dataset from region *A* to recalibrate a model.

As well, this study could be continued with an impact analysis of the selection of spectral neighbours. Both the number of spectral neighbours and the procedure to select them could be analysed. Several approaches are available for selecting representative calibration samples (Shetty et al., 2012) and could also be tested. For example, to analyse the spectral similarity between calibration and test spectra, the Pearson correlation coefficient between spectra could be replaced by the Mahalanobis distance between spectra (Nocita et al., 2014) or the Pearson correlation coefficient distance based on Fast Fourier Transform of spectra (Gogé et al., 2012). Finally, some covariates could be added in local regression to improve prediction accuracy, as previously tested by Nocita et al. (2014) who used clay contents of samples as covariates to predict SOC content.

6. Conclusion

This work highlighted that, as expected, the SOC and SIC contents of French samples were successfully predicted from the French MIRS soil database using a global model based on PLS regression. Predictions of SIC and SOC are accurate when the calibration and validation samples come from same pedologic and climatic contexts. This work also highlighted that when the calibration and validation samples come from different pedologic and climatic contexts, the SOC prediction performance over validation samples decreases, whereas the SIC prediction performance remains accurate. Finally, this work showed that prediction models were more sensitive to the distribution of the explained variables of calibration samples than to the spectral similarity between calibration and test spectra. This study confirmed the very high applicability of MIRS for SIC determination and the robustness of SIC prediction models, even when the calibration and validation samples come from different contexts.

Acknowledgment

RMQS soil sampling and physico-chemical analyses were supported by the GIS Sol, which is a scientific group of interest on soils involving the French Ministry for ecology and sustainable development, the French Ministry of agriculture, the French National institute for geographical and forest information (IGN), the French Environment and Energy Management Agency (ADEME), the French agency for biodiversity, French Institute for Research and Development (IRD) and the French Institute for Agronomic Research (INRA, which is a French public research organisation dedicated to agriculture, food and environment). We thank all the people involved in sampling RMQS sites and in samples preparation. D.A. is coordinator of the Research Consortium GLADSOILMAP, supported by LE STUDIUM Loire Valley Institute for Advanced Studies. And we acknowledge the contribution of three anonymous reviewers for their help in improving the manuscript.

References

Apesteguia, M., Plante, A.F., Virto, I., 2018. Methods assessment for organic and inorganic carbon quantification in calcareous soils of the Mediterranean region. Geoderma Regional 12, 39–48.

Ahmed, Z.U., Woodbury, P.B., Sanderman, J., Hawke, B., Jauss, V., Solomon, D., Lehmann, J., 2017. Assessing soil carbon vulnerability in the Western USA by geospatial modeling of pyrogenic and particulate carbon stocks. Journal of Geophysical Research: Biogeosciences 122, 354–369.

Arrouays, D., Jolivet, C., Boulonne, L., Bodineau, G., Saby, N., Grolleau, E., 2002. A new initiative in France: a multi-institutional soil quality monitoring network. Comptes Rendus de l'Académie d'Agriculture de France 88, 93–105.

Barnes, R.J., Dhanoa, M.S., Lister, S.J., 1989. Standard normal variate transformation and de-trending of near-infrared diffuse reflectance spectra. Applied Spectroscopy. 43, 772–777.

Barthès, B.G., Kouakoua, E., Moulin, P., Hmaidi, K., Gallali, T., Clairotte, M., Bernoux, M., Bourdon, E., Toucet, J., Chevallier, T., 2016. Studying the physical protection of soil carbon with quantitative infrared spectroscopy. Journal of Near Infrared Spectroscopy 24, 199–214.

Batjes, N. H., 1996. Total carbon and nitrogen in the soils of the world. European Journal of Soil Science 47, 151–163.

Bellon-Maurel, V., Fernandez-Ahumada, E., Palagos, B., Roger, J.M., McBratney, A., 2010. Prediction of soil attributes by NIR spectroscopy. A critical review of chemometric indicators commonly used for assessing the quality of the prediction. Trends in Analytical Chemistry (TRAC) 29(9), 1073–1081.

Bellon-Maurel, V., McBratney, A.B., 2011. Near-infrared (NIR) and mid-infrared (MIR) spectroscopic techniques for assessing the amount of carbon stock in soils — Critical review and research perspectives. Soil Biology and Biochemistry 43, 1398–1410.

Bernoux, M., Chevallier, T., 2014. Carbon in Drylands. Multiple Essential Functions. Les Dossier Thématiques du CSFD. N°10. CSFD/Agropolis International, Montpellier, France.

Brown, D.J., Shepherd, K.D., Walsh, M.G., Dewayne Mays, M., Reinsch, T.G., 2006. Global soil characterization with VNIR diffuse reflectance spectroscopy. Geoderma 132, 273–290.

Cécillon, L., Barthès, B.G., Gomez, C., Ertlen, D., Genot, V., Hedde, M., Stevens, A., Brun, J.J., 2009. Assessment and monitoring of soil quality using near-infrared reflectance spectroscopy (NIRS). European Journal of Soil Science 60(5), 770–784.

Chen, Y., Barak, P., 1982. Iron nutrition of plants in calcareous soils. Advances in Agronomy 35, 217–240.

Chong, I.G., Jun, C.H., 2005. Performance of some variable selection methods when multicollinearity is present. Chemometrics and Intelligent Laboratory Systems 78, 103–112.

Clairotte, M., Grinand, C., Kouakoua, E., Thébault, A., Saby, N.P.A., Bernoux, M., Barthès, B.G., 2016. National calibration of soil organic carbon concentration using diffuse infrared reflectance spectroscopy. Geoderma 276, 41–52.

Comstock, J.P., Sherpa, S.R., Ferguson, R., Bailey, S., Beem-Miller, J.P., Lin, F., Lehmann, J., Wolfe, D.W., 2019. Carbonate determination in soils by mid-IR spectroscopy with regional and continental scale models. PLoS ONE 14(2): e0210235.

Dangal, S.R.S., Sanderman, J., Wills, S., Ramirez-Lopez, L., 2019. Accurate and precise prediction of soil properties from a large mid-infrared spectral library. Soil Systems 3, 11.

Dray, S., Dufour, A.B., 2007. The ade4 package: implementing the duality diagram for ecologists. Journal of Statistical Software 22, 1–20.

Du, C., Zhou, J., 2009. Evaluation of soil fertility using infrared spectroscopy: a review. Environmental Chemistry Letters 7, 97–113.

Gogé, F., Joffre, R., Jolivet, C., Ross, I., Ranjard, L., 2012. Optimization criteria in sample selection step of local regression for quantitative analysis of large soil NIRS database. Chemometrics and Intelligent Laboratory Systems 110, 168–176.

Gogé, F., Gomez, C., Jolivet, C., Joffre, R., 2014. Which strategy is best to predict soil properties of a local site from a national Vis–NIR dataset? Geoderma 213, 1–9.

Gregorich E.G., Carter M.R., Angers D.A., Monreal C.M. et Ellert B.H., 1994. Towards a minimum data set to assess soil organic matter quality in agricultural soils. Canadian Journal of Soil Science 74, 367–385.

Grinand, C., Barthès, B.G., Brunet, D., Kouakoua, E., Arrouays, D., Jolivet, C., Caria, G., Bernoux, M., 2012. Prediction of soil organic and inorganic carbon contents at a national scale (France) using mid-infrared reflectance spectroscopy (MIRS). European Journal of Soil Science 63(2), 141–151.

Guerrero, C., Stenberg, B., Wetterlind, J., Viscarra Rossel, R.A., Maestre, F.T., Mouazen, A.M., Zornoza, R., Ruiz-Sinoga, J.D., Kuang, B., 2014. Assessment of soil organic carbon at local scale with spiked NIR calibrations: effects of selection and extra-weighting on the spiking subset. European Journal of Soil Science 65, 248–263.

Guy, A.L., Siciliano, S.D., Lamb, E.G., 2015. Spiking regional vis-NIR calibration models with local samples to predict soil organic carbon in two High Arcticpolar deserts using a vis-NIR probe. Canadian Journal of Soil Science 95, 237–249.

Hannam, K.D., Kehila, D., Millard, P., Midwood, A.J., Neilson, D., Neilson, G.H., Forge, T. A., Nichol, C., Jones, M.D., 2016. Bicarbonates in irrigation water contribute to carbonate formation and CO_2 production in orchard soils under drip irrigation, Geoderma 266, 120–126.

Harris, D., Horwath, W.R., van Kessel, C., 2001. Acid fumigation of soils to remove carbonates prior to total organic carbon or carbon-13 isotopic analysis. Soil Science Society of America Journal 65, 1853–1856.

ISO (International Organization for Standardisation), 1995a. ISO 10693:1995 – Determination of Carbonate Content – Volumetric Method. ISO, Geneva.

ISO (International Organization for Standardisation), 1995b. ISO 10694:1995 - Soil Quality - Determination of Organic and Total Carbon after Dry Combustion (Elementary Analysis). ISO, Geneva.

IUSS Working Group WRB, 2014. International Union of Soil Sciences, Working Group World Reference Base for Soil Resources. World Reference Base for Soil Resources 2014. International Soil Classification System for Naming Soils and Creating Legends of Soil Maps. FAO, Rome.

Jacobson, M., Charlson, R.J., Rodhe, H., Orians, G.H., 2000. Earth System Science: From Biogeochemical Cycles to Global Changes. Academic Press, London.

Jaconi, A., Poeplau, C., Ramirez-Lopez, L., Van Wesemael, B., Don, A., 2019. Log-ratio transformation is the key to determining soil organic carbon fractions with near-infrared spectroscopy. European Journal of Soil Science, 70, 127–139.

Janik, L.J., Skjemstad, J.O., Merry, R.H., 1998. Can mid infrared diffuse reflectance analysis replace soil extractions? Australian Journal of Experimental Agriculture 38, 681–696.

Jauss, V., Sullivan, P.J., Sanderman, J., Smith, D.B., and Lehmann, J., 2017. Pyrogenic carbon distribution in mineral topsoils of the northeastern United States. Geoderma 296, 69–78.

Knadel, M., Deng, F., Thomsen, A., Greve, M.H., 2012. Development of a Danish national vis-NIR soil spectral library for soil organic carbon determination. In: Minasny, B., Malone, B.P., McBratney, A.B. (Eds.), Digital Soil Assessments and Beyond. CRC Press, Boca Raton, FL.

Lagacherie, P., Baret, F., Feret, J.-B., Madeira Netto, J., Robbez-Masson, J.-M., 2008. Estimation of soil clay and calcium carbonate using laboratory, field and airborne hyperspectral measurements. Remote Sensing of Environment 112(3), 825–835.

McCrea, J.M. , 1950. On the isotopic chemistry of carbonates and a paleotemperature scale. Journal of Chemical Physics 18, 849–857.

Mark, H.L., Tunnell, D., 1985. Qualitative near-infrared reflectance analysis using Mahalanobis distances. Analytical Chemistry 57, 1449–1456.

McCarty, G.W., Reeves III, J.B., Reeves, V.B., Follett, R.F., Kimble, J.M., 2002. Mid-infrared and near-infrared diffuse reflectance spectroscopy for soil carbon measurement. Soil Science Society of America Journal 66: 640–646.

Mevik, B.-H., Wehrens, R., 2007. The pls Package: Principal Component and Partial Least Squares Regression in R. Journal of Statistical Software 18, 1–24.

Nocita, M., Stevens, A., Toth, G., Panagos, P., van Wesemael, B., Montanarella, L., 2014. Prediction of soil organic carbon content by diffuse reflectance spectroscopy using a local partial least square regression approach. Soil Biology & Biochemistry 68, 337–347

Pearson, R.K., 2002. Outliers in process modeling and identification. IEEE Transactions on Control Systems Technology 10(1), 55–63.

Pribyl, D.W., 2010. A critical review of the conventional SOC to SOM conversion factor. Geoderma 156, 75–83.

R Development Core Team, 2012. R: A Language and Environment for Statistical Computing. R foundation for Statistical Computing, Vienna. http://www.R-project.org/

Rabenarivo, M., Chapuis-Lardy, L., Brunet, D., Chotte, J.-L., Rabeharisoa, L., Barthès, B.G., 2013. Comparing near and mid-infrared reflectance spectroscopy for determining properties of Malagasy soils, using global or LOCAL calibration. Journal of Near Infrared Spectroscopy 21(6): 495–509.

Ramirez-Lopez, L., Behrens, T., Schmidt, K., Stevens, A., Demattê, J.A.M., Scholten, T. 2013. The spectrum-based learner: A new local approach for modeling soil vis–NIR spectra of complex datasets. Geoderma 195–196, 268–279.

Reeves, D.W., 1997. The role of soil organic matter in maintaining soil quality in continuous cropping systems. Soil & Tillage Research 43, 131–167.

Reeves III, J.B., 2010. Near- versus mid-infrared diffuse reflectance spectroscopy for soil analysis emphasizing carbon and laboratory versus on-site analysis: where are we and what needs to be done? Geoderma 158 (1-2), 3–14.

Romanyà, J., Rovira, P., 2011. An appraisal of soil organic C content in Mediterranean agricultural soils. Soil Use and Management 27, 321–332.

Scharlemann, J.P., Tanner, E.V., Hiederer, R., Kapos, V., 2014. Global soil carbon: understanding and managing the largest terrestrial carbon pool. Carbon Management 5, 81–91.

Shenk, J., Westerhaus, M., Berzaghi, P., 1997. Investigation of a LOCAL calibration procedure for near infrared instruments. J. Near Infrared Spectrosc. 5 (1), 223-232.

Shetty, N., Rinnan, A., Gislum, R., 2012. Selection of representative calibration sample sets fornear-infrared reflectance spectroscopy to predict nitrogen concentration in grasses. Chemometrics and Intelligent Laboratory Systems 111, 59–65.

Shi, Z., Ji, W., Viscarra-Rossel, R.A., Chen, S., Zhou, Y., 2015. Prediction of soil organic matter using a spatially constrained local partial least squares regression and the Chinese vis–NIR spectral library. European Journal of Soil Science 66, 679–687.

Soriano-Disla, J.M., Janik, L.J., Viscarra Rossel, R.A., MacDonald, L.M., McLaughlin, M.J., 2014. The performance of visible, near-, and mid-infrared reflectance spectroscopy for prediction of soil physical, chemical, and biological properties. Applied Spectroscopy Reviews 49(2), 139–186.

Stevens, A, Nocita, M, Tóth, G, Montanarella, L, van Wesemael, B., 2013. Prediction of soil organic carbon at the European scale by visible and near infrared reflectance spectroscopy. PLoS ONE 8(6): e66409.

Tatzber, M., Mutsch, F., Mentler, A., Leitger, E., Englich, M., Gerzabek, M., 2010. Determination of organic and inorganic carbon in forest soil samples by mid-infrared spectroscopy and partial least squares regression. Applied Spectroscopy 64(10):1167–75.

Tenenhaus, M., 1998. La Régression PLS. Editions Technip, Paris.

Terra, F.S., Demattê, J.A.M., Viscarra Rossel R.A. (2015). Spectral libraries for quantitative analyses of tropical Brazilian soils: Comparing vis–NIR and mid-IR reflectance data. Geoderma 255–256 (2015) 81–93

Viscarra Rossel, R.A., Jeon, Y.S., Odeh, I.O.A., McBratney, A.B., 2008. Using a legacy soil sample to develop a mid-IR spectral library. Soil Research 46, 1–16.

Viscarra Rossel, R.A., Walvoort, D.J.J., Mc Bratney, A.B., Janik, L.J., Skjemstad, J.O., 2006. Visible, near-infrared, mid-infrared or combined diffuse reflectance spectroscopy for simultaneous assessment of various soil properties. Geoderma 131, 59–75.

Viscarra Rossel, R.A., Webster, R., 2012. Predicting soil properties from the Australian soil visible-near infrared spectroscopic database. European Journal of Soil Science 63, 848–860.

Viscarra Rossel, R.A., Behrens, T., Ben-Dor, E., Brown, D.J., Demattê, J.A.M., Shepherd, K.D., Shi, Z., Stenberg, B., Stevens, A., Adamchuk, V., Aïchi, H., Barthès, B.G., Bartholomeus, H.M., Bayer, A.D., Bernoux, M., Böttcher, K., Brodsky, L., Du, C.W., Chappell, A., Fouad, Y., Genot, V., Gomez, C., Grunwald, S., Gubler, A., Guerrero, C., Hedley, C.B., Knadel, M., Morras, H.J.M., Nocita, M., Ramirez-Lopez, L., Roudier, P., Campos, E.M. Rufasto, Sanborn, P., Sellitto, V.M., Sudduth, K.A., Rawlins, B.G., Walter, C., Winowiecki, L.A., Hong, S.Y., Ji, W., 2016. A global spectral library to characterize the world's soil. Earth-Science Reviews 155, 198–230.

Viscarra Rossel, R.A., Lark, R.M., 2009, Improved analysis and modelling of soil diffuse reflectance spectra using wavelets. European Journal of Soil Science 60, 453–464.

Vohland, M., Ludwig, M., Harbich, M., Emmerling, C., Thiele-Bruhn, S., 2016. Using variable selection and wavelets to exploit the full potential of visible–near infrared spectra for predicting soil properties. Journal of Near Infrared Spectroscopy 24, 255–269.

Walkley, A., Black, I.A., 1934. An examination of the Degtjareff method for determining soil organic matter, and a proposed modification of the chromic acid titration method. Soil Science 37(1), 29–38.

Wang, X., Wang, J., Zhang, J. (2012) Comparisons of three methods for organic and inorganic carbon in calcareous soils of northwestern China. PLoS ONE 7(8): e44334.

Wijewardane, N.K., Ge, Y., Wills, S., Libohova, Z., 2018. Predicting physical and chemical properties of US soils with a mid-infrared reflectance spectral library. Soil Science Society of America Journal 82, 722–731

Williams, P.C., Norris, K.H., 1987. Qualitative applications of near-infrared reflectance spectroscopy. In: Williams, P., Norris, K. (Eds.), Near-Infrared Technology in the Agricultural and Food Industries. American Association of Cereal Chemists, St. Paul, MN, pp. 241–246.

Wold, S., Johansson, E., Cocchi, M., 1993. PLS - partial least squares projections to latent structures. In: Kubinyi, H. (Ed.), 3D-QSAR in Drug Design, Theory, Methods, and Applications. ESCOM Science Publishers, Leiden, pp. 523–550.

Wold, S., Sjöström, M., Eriksson, L., 2001. PLS-regression: a basic tool of chemometrics. Chemometrics and Intelligent Laboratory Systems 58, 109–130.

Workman, J. Jr.,, Weyer, L., 2008. Practical Guide to Interpretive Near-Infrared Spectroscopy. CRC Press, Boca Raton, FL.

Waruru, B.K., Shepherd K.D., Ndegwa G.M., Kamoni P.T., Sila A.M. 2014. Rapid estimation of soil engineering properties using diffuse reflectance near infrared spectroscopy. Biosystems Engineering, 121, pp. 177-185.

Yang, M., Xu, D., Chen, S., Li, H., Shi, Z., 2019. Evaluation of machine learning approaches to predict soil organic matter and pH using vis-NIR spectra. Sensors 19, 263.

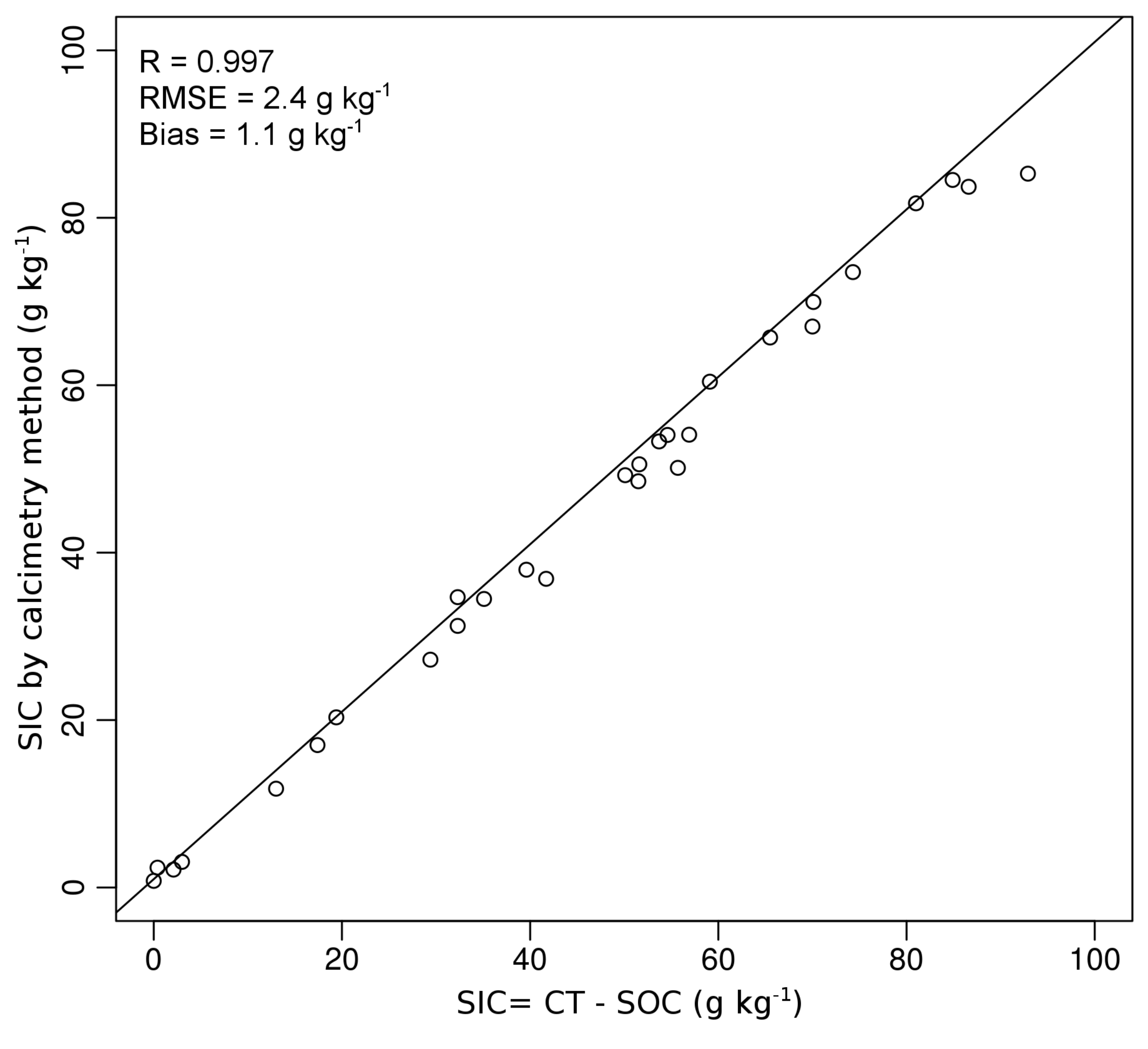

R = 0.997
RMSE = 2.4 g kg-1
Bias = 1.1 g kg-1
SIC by calcimetry method (g kg-1)
SIC= CT - SOC (g kg-1)
0
20
40
60
80
100

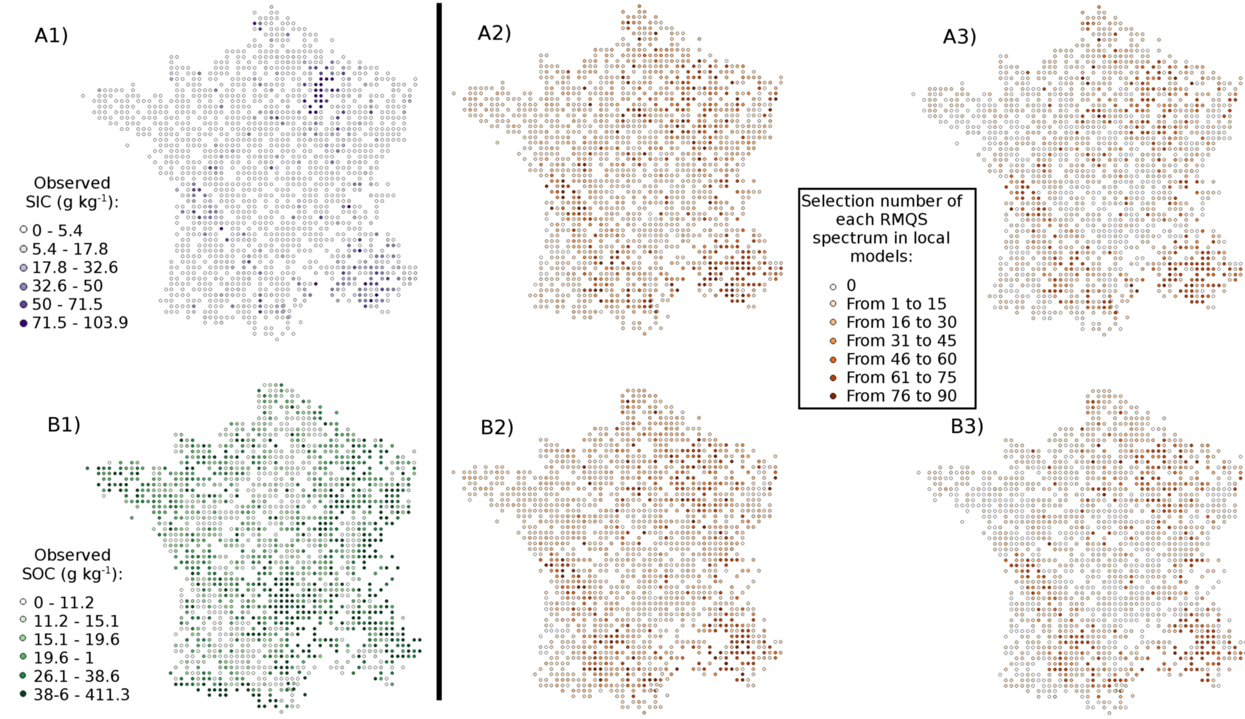
A1)
Observed SIC (g kg-1):
0 - 5.4
5.4 - 17.8
17.8 - 32.6
32.6 - 50
50 - 71.5
71.5 - 103.9
A2)
A3)
Selection number of each RMQS spectrum in local models:
0
From 1 to 15
From 16 to 30
From 31 to 45
From 46 to 60
From 61 to 75
From 76 to 90
B1)
Observed SOC (g kg-1):
0 - 11.2
11.2 - 15.1
15.1 - 19.6
19.6 - 1
26.1 - 38.6
38-6 - 411.3
B2)
B3)

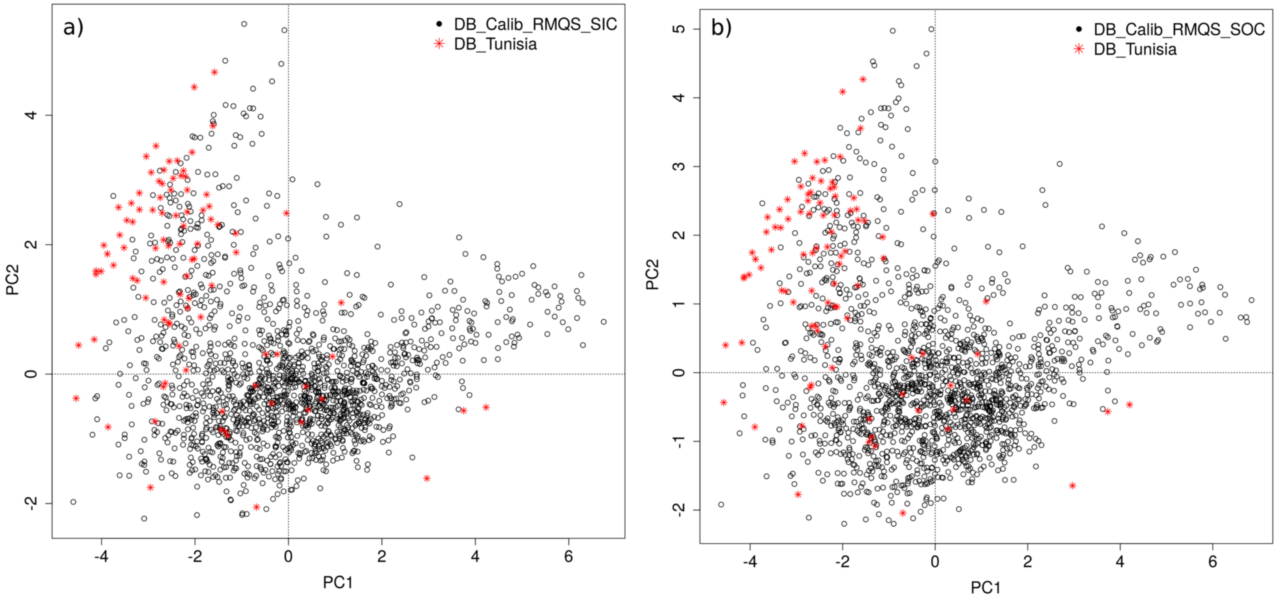

a)
DB_Calib_RMQS_SIC
DB_Tunisia
PC1
PC2
b)
DB_Calib_RMQS_SOC
DB_Tunisia
PC1
PC2

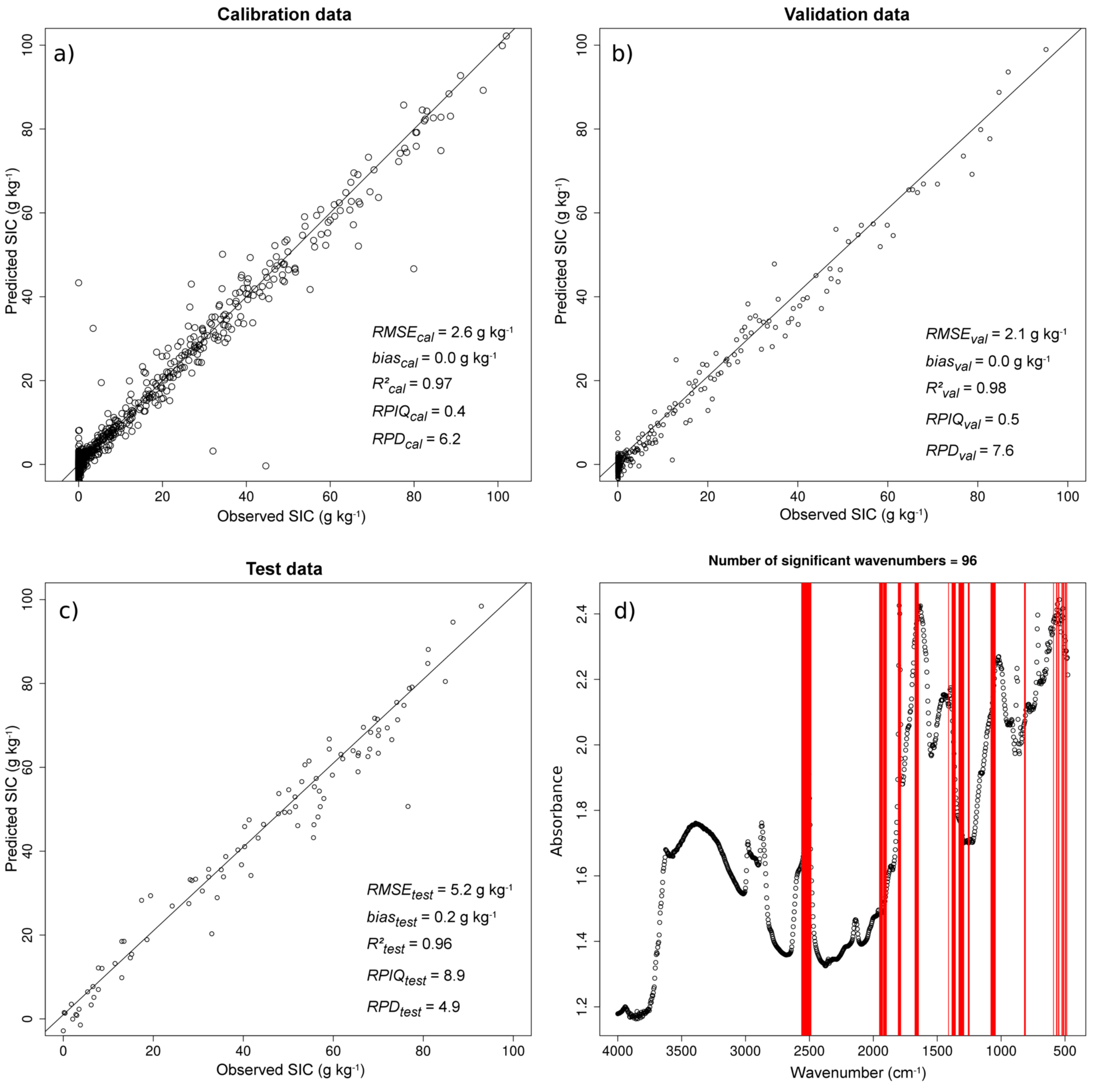
Calibration data
a)
Predicted SIC (g kg-1)
Observed SIC (g kg-1)
RMSEcal = 2.6 g kg-1
biascal = 0.0 g kg-1
R²cal = 0.97
RPIQcal = 0.4
RPDcal = 6.2
Validation data
b)
RMSEval = 2.1 g kg-1
biasval = 0.0 g kg-1
R²val = 0.98
RPIQval = 0.5
RPDval = 7.6
Test data
c)
RMSEtest = 5.2 g kg-1
biastest = 0.2 g kg-1
R²test = 0.96
RPIQtest = 8.9
RPDtest = 4.9
Number of significant wavenumbers = 96
d)
Absorbance
Wavenumber (cm-1)

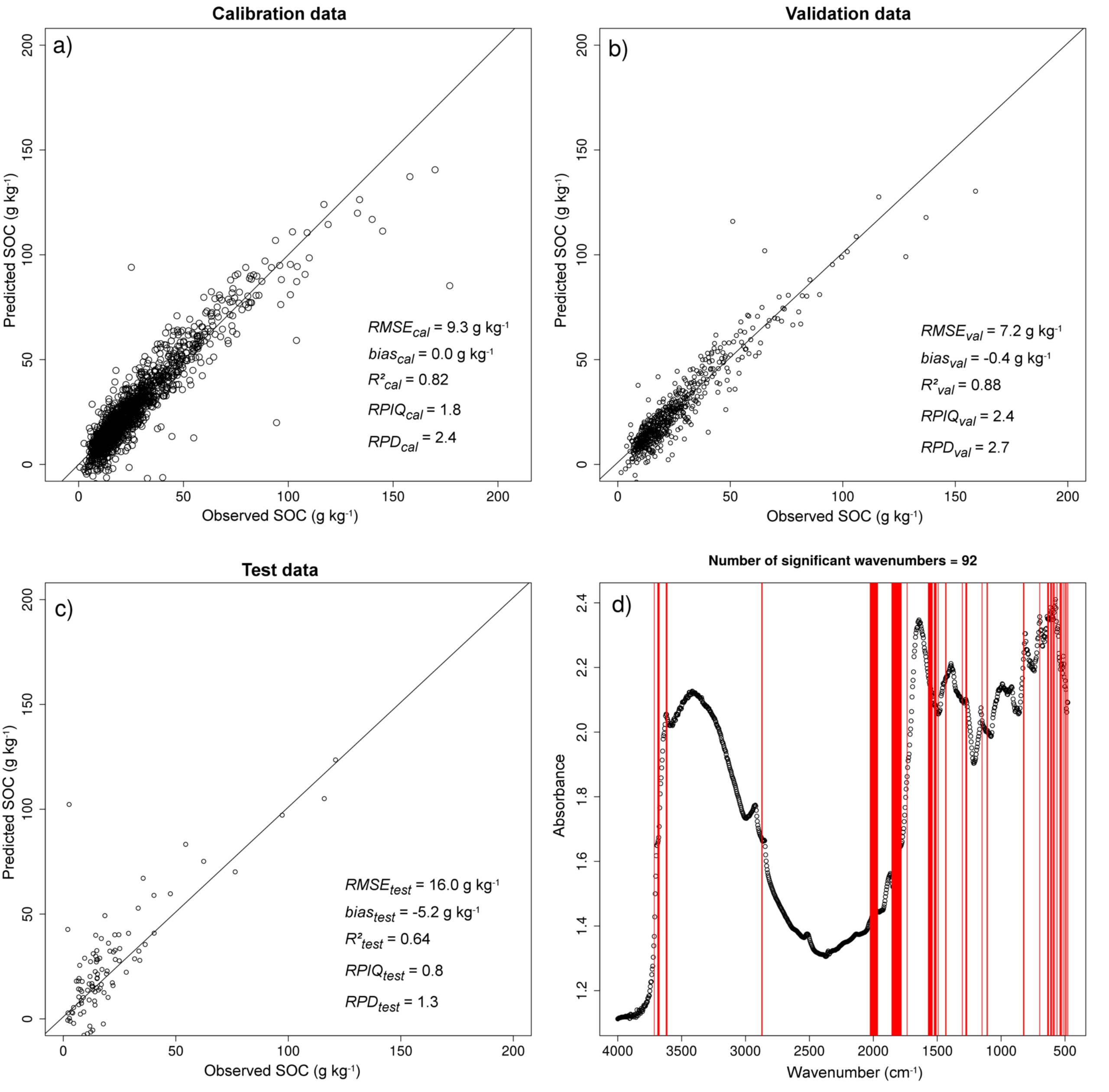
Calibration data
a)
$RMSE_{cal}$ = 9.3 g kg^{-1}
$bias_{cal}$ = 0.0 g kg^{-1}
R^2_{cal} = 0.82
$RPIQ_{cal}$ = 1.8
RPD_{cal} = 2.4
Predicted SOC (g kg^{-1})
Observed SOC (g kg^{-1})
Validation data
b)
$RMSE_{val}$ = 7.2 g kg^{-1}
$bias_{val}$ = -0.4 g kg^{-1}
R^2_{val} = 0.88
$RPIQ_{val}$ = 2.4
RPD_{val} = 2.7
Predicted SOC (g kg^{-1})
Observed SOC (g kg^{-1})
Test data
c)
$RMSE_{test}$ = 16.0 g kg^{-1}
$bias_{test}$ = -5.2 g kg^{-1}
R^2_{test} = 0.64
$RPIQ_{test}$ = 0.8
RPD_{test} = 1.3
Predicted SOC (g kg^{-1})
Observed SOC (g kg^{-1})
Number of significant wavenumbers = 92
d)
Absorbance
Wavenumber (cm^{-1})

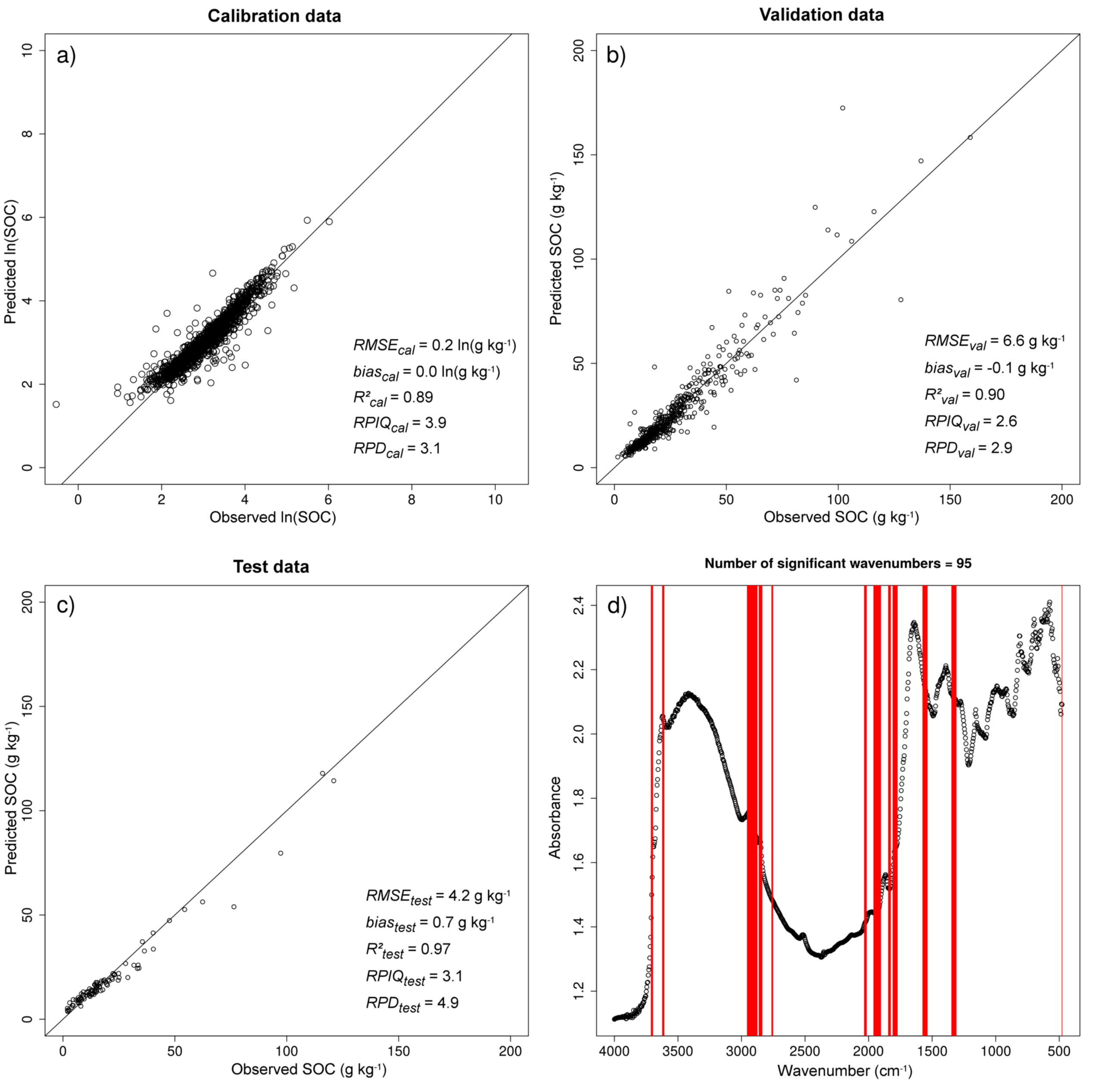

Calibration data
a)
Predicted ln(SOC)
Observed ln(SOC)
RMSE_cal = 0.2 ln(g kg-1)
bias_cal = 0.0 ln(g kg-1)
R²_cal = 0.89
RPIQ_cal = 3.9
RPD_cal = 3.1
Validation data
b)
Predicted SOC (g kg-1)
Observed SOC (g kg-1)
RMSE_val = 6.6 g kg-1
bias_val = -0.1 g kg-1
R²_val = 0.90
RPIQ_val = 2.6
RPD_val = 2.9
Test data
c)
Predicted SOC (g kg-1)
Observed SOC (g kg-1)
RMSE_test = 4.2 g kg-1
bias_test = 0.7 g kg-1
R²_test = 0.97
RPIQ_test = 3.1
RPD_test = 4.9
Number of significant wavenumbers = 95
d)
Absorbance
Wavenumber (cm-1)

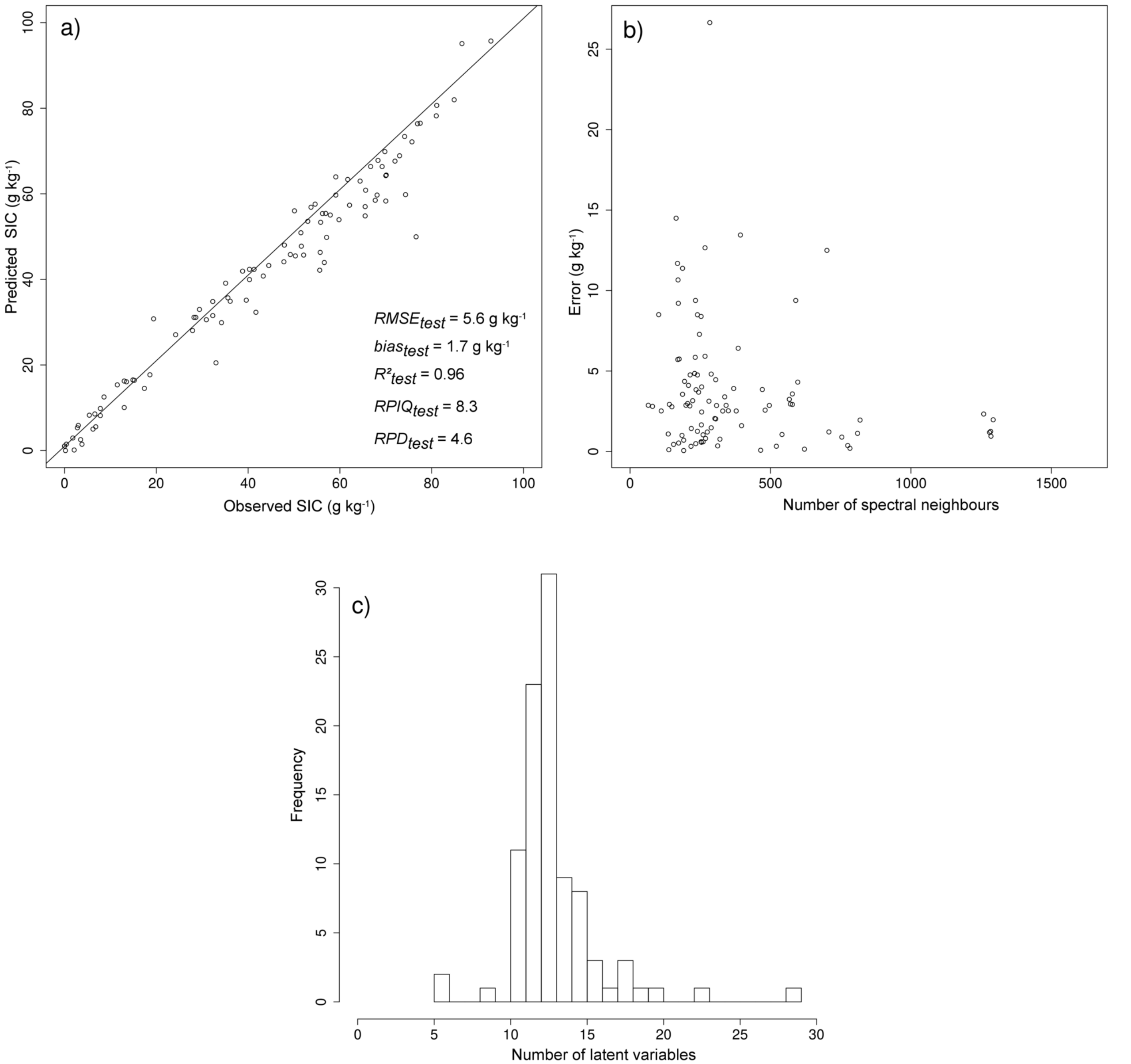

a)
Predicted SIC (g kg-1)
Observed SIC (g kg-1)
RMSEtest = 5.6 g kg-1
biastest = 1.7 g kg-1
R²test = 0.96
RPIQtest = 8.3
RPDtest = 4.6
b)
Error (g kg-1)
Number of spectral neighbours
c)
Frequency
Number of latent variables

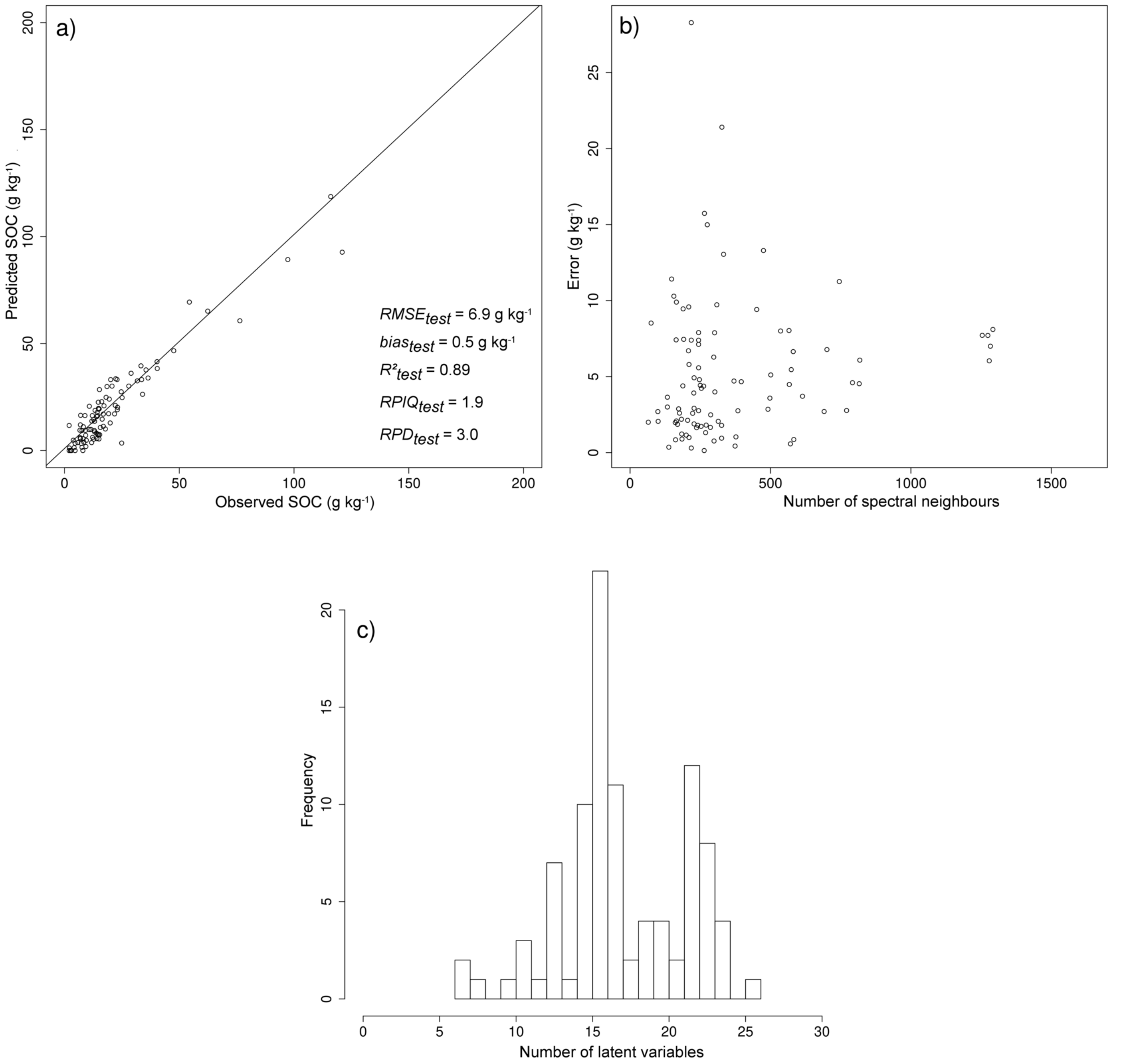
a)
Predicted SOC (g kg-1)
Observed SOC (g kg-1)
0
50
100
150
200
RMSEtest = 6.9 g kg-1
biastest = 0.5 g kg-1
R²test = 0.89
RPIQtest = 1.9
RPDtest = 3.0
b)
Error (g kg-1)
Number of spectral neighbours
0
5
10
15
20
25
500
1000
1500
c)
Frequency
Number of latent variables
0
5
10
15
20
25
30

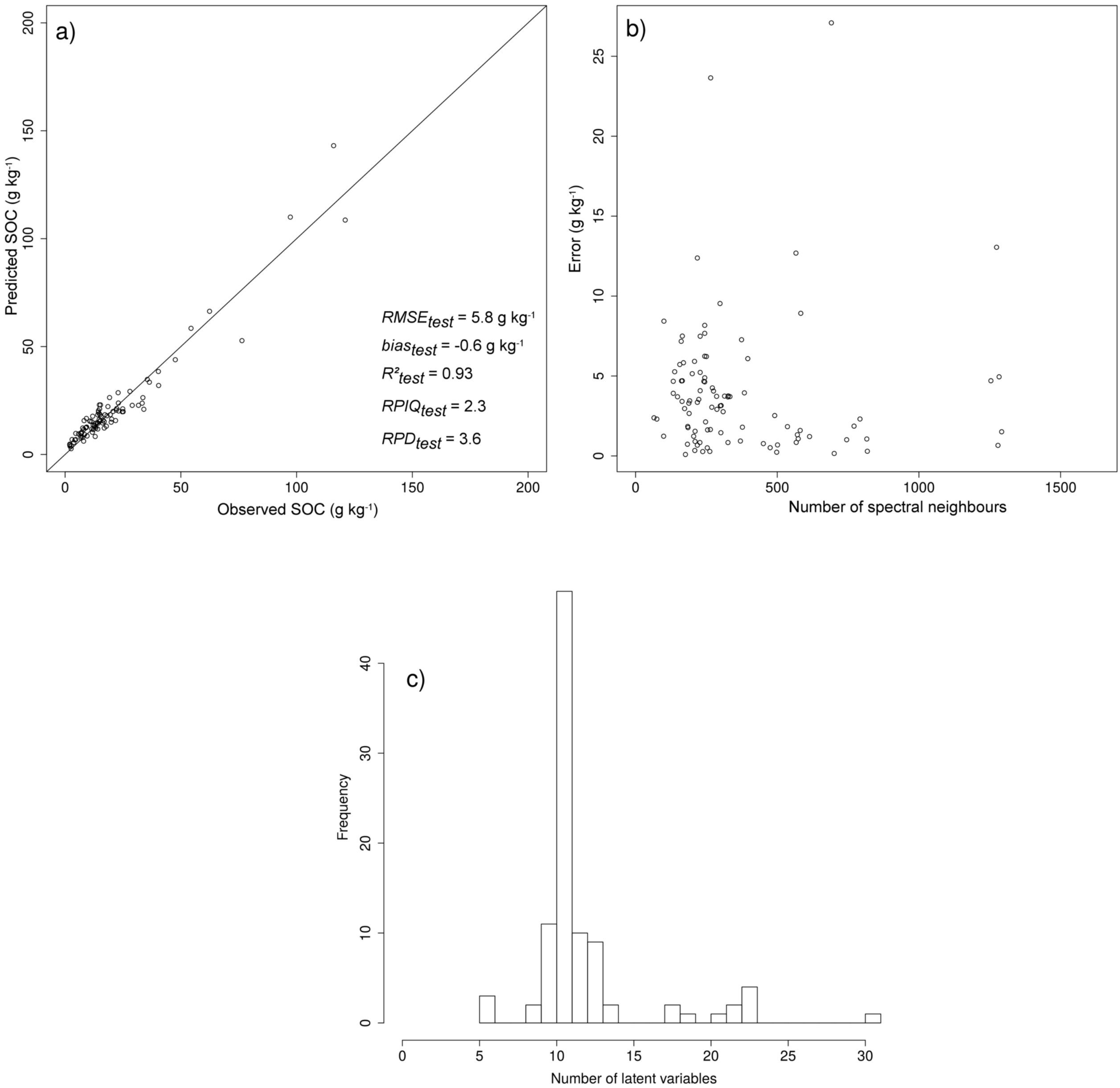
a)
Predicted SOC (g kg-1)
Observed SOC (g kg-1)
RMSEtest = 5.8 g kg-1
biastest = -0.6 g kg-1
R²test = 0.93
RPIQtest = 2.3
RPDtest = 3.6
0
50
100
150
200
b)
Error (g kg-1)
Number of spectral neighbours
0
5
10
15
20
25
500
1000
1500
c)
Frequency
Number of latent variables
0
10
20
30
40
5
15
25

Table 1: Soil datasets statistics. The SIC values set to zero correspond to values under the laboratory quantification limit (< 0.1 g kg^{-1}).

Dataset	Number of soil samples	Min g kg^{-1}	Max g kg^{-1}	Mean g kg^{-1}	Median g kg^{-1}	SD[a] g kg^{-1}	Skewness
DB_RMQS_SOC	2178	0.6	411.3	25.8	19.6	21.8	4.9
DB_RMQS_SIC	2178	0.0	103.9	6.4	0.0	16.1	3.1
DB_Tunisia_SOC	96	2.0	121.0	20.1	14.6	21.0	3.0
DB_Tunisia_SIC	96	0.0	92.9	43.3	48.5	25.6	-0.2
DB_Calib_RMQS_SOC	1586[b]	0.6	411.3	25.6	19.4	22.3	5.5
DB_Calib_RMQS_SIC	1582[c]	0.0	103.9	6.4	0	16.1	3.1
DB_Valid_RMQS_SOC	544	1.5	159.0	25.5	19.6	19.5	2.5
DB_Valid_RMQS_SIC	544	0.0	95.2	6.3	0.0	15.7	3.1

[a] SD: standard deviation

[b] after removing 48 spectral outliers

[c] after removing 52 spectral outliers

Table 2: Figures of merit obtained with global and local models over the French calibration and validation databases.

Models	R^2_{cv}	*RMSECV* (g kg^{-1})	R^2_{val}	$RMSE_{val}$ (g kg^{-1})	$bias_{val}$ (g kg^{-1})	RPD_{val}	$RPIQ_{val}$
$\boldsymbol{GM_{SIC}}$	0.97	2.8	0.98	2.1	0.0	7.6	0.5
$\boldsymbol{LM_{SIC}}$	*nd*	*nd*	0.99	1.8	0.0	8.8	0.6
$\boldsymbol{GM_{SOC}}$	0.80	9.9	0.88	7.2	-0.4	2.7	2.4
$\boldsymbol{LM_{SOC}}$	*nd*	*nd*	0.93	5.4	-0.7	3.6	3.2
$\boldsymbol{GM_{lnSOC}}$	0.89	0.2*	0.90	6.6	-0.1	2.9	2.6
$\boldsymbol{LM_{lnSOC}}$	*nd*	*nd*	0.92	5.7	-0.1	3.4	3

**RMSEcv calculated on ln(SOC)*

nd: Not determined.

Table 3: Figures of merit obtained with global and local models over the Tunisian soil samples.

Prediction model	R^2_{test}	$RMSE_{test}$ (g kg^{-1})	$bias_{test}$ (g kg^{-1})	RPD_{test}	$RPIQ_{test}$
$\boldsymbol{GM_{SIC}}$	0.96	5.2	0.2	4.9	8.9
$\boldsymbol{LM_{SIC}}$	0.96	5.6	1.7	4.6	8.3
$\boldsymbol{GM_{SOC}}$	0.64	16.0	-5.2	1.3	0.8
$\boldsymbol{LM_{SOC}}$	0.89	6.9	0.5	3.0	1.9
$\boldsymbol{GM_{lnSOC}}$	0.97	4.2	0.7	4.9	3.1
$\boldsymbol{LM_{lnSOC}}$	0.93	5.8	-0.6	3.6	2.3